FCP Report No. 38

AN ANALYTICAL STUDY OF THE FATIGUE NOTCH SIZE EFFECT

by

P. K. Mazumdar
Department of Metallurgy and Mining Engineering

and

F. V. Lawrence, Jr.
Professor of Civil Engineering and Metallurgy

A Report of the
FRACTURE CONTROL PROGRAM
College of Engineering, University of Illinois
Urbana, Illinois 61801
April, 1981

AN ANALYTICAL STUDY OF THE FATIGUE NOTCH SIZE EFFECT

ABSTRACT

An analytical expression for K_f in terms of notch depth (A), elastic stress concentration factor (K_t) and initiated crack length (a_I) has been developed. Together with the strain-controlled fatigue concepts and the Newman's stress intensity correction factor solution, the expression for K_f was used to study the notch-size effect and other phenomena related to the notch-size effect. Results of this study indicate that the notched specimen behavior was best represented by Peterson's equation rather than Neuber's equation. The material constant (a) based on Peterson's equation, for steels and aluminum alloys, was related to the strain-controlled fatigue properties and the fatigue crack propagation parameters.

Conditions for which nonpropagating fatigue cracks will form was studied using the present model. The analytical expression for K_f was used to evaluate the length of the nonpropagating cracks as a function of the stress level. A universal plot based on the theories developed for notched specimens is proposed that well describes the behavior of cracked specimens. The intrinsic crack length (ℓ_0) proposed by Haddad et al. could be related to the material constant (a).

Analytical estimates were compared with the experimental results taken from the literature and a good agreement was observed.

ACKNOWLEDGMENTS

This study was principally supported by the University of Illinois Fracture Control Program which is funded by a consortium of midwest industries.

The authors wish to thank Professors JoDean Morrow of the Department of Theoretical and Applied Mechanics and D. F. Socie of the Department of Mechanical and Industrial Engineering for their suggestions and discussions.

The authors are thankful to Mrs. Darlene Mathine and Mrs. Marrianne Day for their patience in carefully typing the manuscript.

TABLE OF CONTENTS

LIST OF TABLES

LIST OF FIGURES

LIST OF SYMBOLS

a and ρ	Material constant relating K_f to K_t and r based on Peterson and Neuber equations
a_I	Nonarbitrarily defined crack initiation length
a_{th}	Crack length resulting in a stress intensity
	Factor range equal to ΔK_{th}
A	Half major-axis of an elliptical notch
b	Fatigue strength exponent; also, half minor-axis of an elliptical notch
B	Exponent of the equation relating q, a and r
c	Half notch depth plus half crack length
E	Young's modulus
F	Stress intensity correction factor
K	Stress intensity factor
ΔK_{th}	Threshold stress intensity factor
K_f	Fatigue notch factor
K_t	Theoretical stress concentration factor
ℓ	Half the crack length, also length of an edge crack
ℓ_o	Intrinsic crack length
$2N_f$	Number of reversals to failure
N_f	Total life - number of cycles to failure
N_I	Number of cycles necessary to initiate a crack
N_P	Number of cycles necessary to propagate a crack after initiation to final fracture
q	Fatigue notch sensitivity index
R	Load ratio

r	Notch root radius
S, ΔS	Nominal stress, range
S_a, ΔS_a	Nominal fatigue strength amplitude of smooth specimen
S_c, ΔS_c	Nominal fatigue strength amplitude and range for cracked specimen
S_i	Nominal stress amplitude to initiate a crack
S_n	Nominal stress amplitude of notched specimen
S_y	Yield strength
S_u	Ultimate tensile strength
x	Distance from the notch root
σ'_f	Fatigue strength coefficient
β	Gradient of the plot at $X = 0$ relating normalized product of the stress-strain distribution to normalized distance ahead of a notch root
α	Constant of the equation relating β to $(K_t - 1)$
γ	Exponent of the equation relating β to $(K_t - 1)$
$N(o)$	$[\Delta\sigma(o)\ \Delta\varepsilon(o)\ E]^{\frac{1}{2}}$ stress-strain parameter at notch root
$N(\ell/A)$	$[\Delta\sigma(\ell/A)\ \Delta\varepsilon(\ell/A)\ E]^{\frac{1}{2}}$ stress-strain parameter at the initiated fatigue element (ℓ) from the notch root
$N(\infty/A)$	$[\Delta\sigma(\infty/A)\ \Delta\varepsilon(\infty/A)\ E]^{\frac{1}{2}}$ nominal stress-strain parameter
$N(x/A)$	$[\Delta\sigma(x/A)\ \Delta\varepsilon(x/A)\ E]^{\frac{1}{2}}$ stress-strain parameter experienced by the fatigue element at a distance x from the notch root

1. INTRODUCTION

1.1 General

In order to make engineering predictions of fatigue life, it is convenient to separate the total fatigue life (N_f) of an element into two parts: the crack initiation life (N_I) and the crack propagation life (N_p). N_I is considered to consist of the number of cycles for crack nucleation (caused by repeated shear strains), crystallographically oriented crack growth and coalescence of several small cracks into a dominant, propagating fatigue crack of initiated crack length, a_I. N_p is considered to consist of the cycles devoted to stable crack growth from the initiated crack length (a_I) to final fracture. Because the crack initiation is different from the crack propagation process (1)[+], separate methods of analysis have been developed for predicting the crack initiation and crack propagation lives. Generally, strain-controlled fatigue concepts are used to predict the initiation life, and fracture mechanics concepts are used to predict the propagation life.

1.2 Fatigue at Notches

The presence of notches and other stress raisers is almost unavoidable in engineering practice, and a substantial effort has been devoted to devising methods for predicting the fatigue strength of a notched element from the behavior of unnotched, laboratory specimens.

The fatigue notch factor (K_f), a strength reduction factor in fatigue, is defined as the ratio of the unnotched to notched specimen fatigue strength

---

[+]The numbers in parentheses refer to the list of references at the end of the text.

at a given life and is always less than or equal to the value of the theoretical stress concentration factor (K_t). For geometrically similar notches, K_f (unlike K_t) depends upon the absolute size of the notch: this effect is known as the notch size effect (2-15).

The notch size effect is often quantified by the notch sensitivity index (q):

$$q = \frac{(K_f - 1)}{(K_t - 1)} \tag{1}$$

The value of q is a function of both the material tested and the notch root radius (r) and varies between zero (when the material experiences no reduction in fatigue strength due to a notch, i.e. $K_f = 1$) and one (when the material experiences the full theoretical effect of a notch, i.e. $K_f = K_t$).

There is a great deal of fatigue test data in the literature for notched specimens from which several relationships between K_f and K_t have been developed. These relationships have been reviewed by Yen et al. (16) and have also been conveniently summarized by Frost et al. (17). Though such relationships are essentially empirical, they are useful in design. Among the relationships between K_f and K_t, Neuber's (2) and Peterson's (5,6) equations are most commonly used.

Neuber considered a material to be composed of "building blocks" of finite dimension (ρ) that is a constant for each material. Neuber's explanation of the size effect is based on the breakdown of the theory of elasticity as the notch root radius (r) approaches the size of these "building blocks" due to the increasingly large stress gradients and the material's microscopic anisotropy and inhomogeneity. From this concept, Neuber developed the following expression for K_f at notches:

$$K_f = 1 + \frac{K_t - 1}{1 + \left(\frac{\rho}{r}\right)^{\frac{1}{2}}} \tag{2}$$

where: ρ = experimentally determined material constant.

The material constant (ρ) has been shown to decrease with an increase in ultimate tensile strength (S_u) for both steels and aluminum alloys (4).

Peterson interpreted the fatigue notch size effect in terms of the stress gradient ahead of the notch and a distance (δ) that is a characteristic of a particular material. Peterson assumed that fatigue failure occurs when the stress at a distance (δ) ahead of the notch (K_f S) equals the endurance limit of an unnotched specimen. This assumption leads to the result called Peterson's equation:

$$K_f = 1 + \frac{K_t - 1}{1 + \left(\frac{a}{r}\right)} \tag{3}$$

where: a = experimentally determined material constant.

For design purposes the material constant (a) for steel is (18):

$$a = 0.001\left(\frac{300}{S_u}\right)^{1.8} \text{ in.} \tag{4}$$

In general, Eqs. 2 and 3 may be written in the following form:

$$K_f = 1 + \frac{K_t - 1}{1 + \left(\frac{a}{r}\right)^B} \tag{5}$$

where: B = $\frac{1}{2}$ for Neuber's equation

1 for Peterson's equation

and a = material constant (for Peterson's equation and should be replaced by ρ for Neuber's equation)

Using Eq. 5, the fatigue notch sensitivity (q) (Eq. 1) becomes:

$$q = \frac{1}{\left[1 + \left(\frac{a}{r}\right)^{B}\right]} \tag{6}$$

Conventionally, the material constant is evaluated by fitting the experimental data in q versus log r plots (Fig. 1a) using an adjustable parameter (a or ρ). However, Eq. 6 may be written as:

$$\frac{(1 - q)}{q} = \left(\frac{a}{r}\right)^{B} \tag{7}$$

Therefore, a plot of log $\{(1 - q)/q\}$ versus log 1/r (Fig. 1b) will be easy to interpret and will be used in this study since the slope from such a plot is B and the inverse of (1/r) at $\{(1 - q)/q\} = 1$ is the value of the material constant (a or ρ).

1.3 Limiting or Maximum Values of K_f

Both Neuber and Peterson's equations are widely used in engineering design, but different values of K_f result for a material with a given notch unless $a/r = (\rho/r)^{\frac{1}{2}}$, a condition that is seldom met. The present study has attempted to determine whether a material should follow Neuber's or Peterson's equation. As will be seen, answering this question has far reaching theoretical and practical implications.

For an elliptical notch in an infinite plate, K_t is:

$$K_t = 1 + 2\left(\frac{A}{r}\right)^{\frac{1}{2}} \tag{8}$$

where: A = half the notch depth

r = notch root radius

Combining the Neuber equation (Eq. 2) for elliptical notches and Eq. 8 leads to:

$$K_f = 1 + \frac{2\left(\frac{A}{r}\right)^{\frac{1}{2}}}{1 + \left(\frac{\rho}{r}\right)^{\frac{1}{2}}} \tag{9}$$

For elliptical notches of given depth, Eq. 9 predicts that K_f should increase as r decreases (dashed line in Fig. 2) and reaches a limiting value ($K_{f,lim}$) as r approaches zero:

$$K_{f,lim} = 1 + 2\left(\frac{A}{\rho}\right)^{\frac{1}{2}} \tag{10}$$

$K_{f,lim}$ is the highest value of K_f that can be achieved for a notch of given depth (A) using Neuber's equation, and its magnitude is dependent on ρ.

Similarly, combining Peterson's equation (Eq. 3) with Eq. 8:

$$K_f = 1 + \frac{2\left(\frac{A}{r}\right)^{\frac{1}{2}}}{1 + \left(\frac{a}{r}\right)} \tag{11}$$

Equation 11 predicts that K_f should approach one as r approaches zero; but K_f passes through a maximum (19) at some critical value of r equal to (a) (solid line in Fig. 2):

$$r_c = a \tag{12}$$

The value of $K_{f,max}$ is:

$$K_{f,max} = 1 + \left(\frac{A}{a}\right)^{\frac{1}{2}} \tag{13}$$

For a given material $K_{f,max}$ is the highest value of K_f that can be achieved by a notch of given depth (A) based on Peterson's equation, and its magnitude is dependent on (a).

Thus, the use of the Neuber and Peterson equations (Eqs. 9 and 11) result in the estimation of quite different values of K_f for sharp notches (Fig. 2), particularly under elastic conditions. The predicted fatigue strength computed on the basis of Neuber's equation would be lower than the strength based on Peterson's equation, since, in general, $a/r > (\rho/r)^{\frac{1}{2}}$. Thus, one wonders:

(i) Which of these equations best characterizes a material's behavior?

(ii) Are the material constants really a function of the material or do they depend also on other variables such as notch depth (a), etc?

The above questions are important since the concept of $K_{f,max}$ is very useful for predicting the fatigue strength of notched and welded components. The answering of these questions will be the principal purpose of the present study.

1.4 Scope

In the present study, an analytical model is proposed for K_f which is a function of K_t and the initiated crack length (a_I). The use of this equation for K_f together with the Newman's stress-intensity-correction-factor solution for two cracks emanating from an elliptical notch (20) and strain-controlled fatigue concepts (21) permits the study of the notch size effect in a systematic way. The present study is restricted to elliptical notches in an infinite plate subjected to completely reversed axial loading under plane stress conditions and a failure life (N_f) of 10^7 cycles.

In addition, the developed equation for K_f will be used to examine the conditions for the formation of the nonpropagating cracks and to evaluate the maximum length of such nonpropagating cracks in a notched specimen.

2. ANALYTICAL MODEL

2.1 General

An analytical model for K_f in terms of the notch depth (A), elastic stress concentration factor (K_t) and the initiated crack length (a_I) was developed:

$$(K_f - 1) = (K_t - 1) \exp - (K_t - 1)^{1.5} \left(\frac{a_{th}}{A}\right) \tag{14}$$

The following sections describe the development of this model for K_f and its use in conjunction with the Newman's stress-intensity-correction-factor solution in an infinite plate with two cracks emanating from an elliptical notch (20) and with the strain-controlled properties (21) to predict the many phenomena associated with the notch-size effect.

2.2 Concept of the Initiated Crack Length (a_I)

Two recent studies (22,23) have proposed a nonarbitrary definition of the initiated crack length (a_I). In these studies, estimates of a_I are based on the fatigue history experienced by the elements ahead of a notch root (Fig. 3a). The Rate Calculation Method (22) defines a_I as that element ahead of a notch root for which the damage rate due to crack initiation and crack propagation are equal. The Total Life Calculation Method (23) defines a_I as that distance to that element ahead of a notch root for which the total life is a minimum (Fig. 3b). For constant amplitude loading, both techniques have been shown to be equivalent (23), and the Total Life Calculation model will be used herein because of its simplicity.

At high stresses, N_f becomes minimum at a value of a_I (solid arrow in Fig. 4) which is greater than a_{th} (open arrow). At low stresses, the minimum

N_f has been found to occur at values of a_I which approach a_{th} (Fig. 4c). Thus, at low stresses, ΔK_{th} would determine a_I (i.e., a_{th}). Physically, this result is interpreted as meaning that the element a_I (a_{th}) would fail faster through the accumulation of fatigue crack initiation damage than by the propagation of an existing fatigue crack of size less than a_{th} to a_{th} (see Fig. 5).

2.3 Model for Fatigue Notch Factor (K_f)

The expression (Eq. 14) developed for the fatigue notch factor (K_f) is based on crack initiation and an analytical model for the stress-strain distribution at elliptical notches. The normalized stress-strain distribution ahead of an elliptical notch root has been shown to depend solely on K_t (Eq. A-5 in Appendix):

$$\frac{N\left(\frac{x}{A}\right)}{N\left(\frac{\infty}{A}\right)} - 1 = (K_t - 1) \exp - (K_t - 1)^{1.5} \left(\frac{x}{A}\right) \qquad (15)$$

where: $N(x/A) = [\Delta\sigma(x/A)\ \Delta\varepsilon(x/A)\ E]^{\frac{1}{2}}$, stress-strain parameter ahead of a notch root as a function of the distance (x)

$N(\infty/A) = [\Delta\sigma(\infty/A)\ \Delta\varepsilon(\infty/A)\ E]^{\frac{1}{2}}$, nominal stress-strain parameter

Since ΔK_{th} determines a_I at lower stresses (Section 2.2, Fig. 5), the element (x/A) (Figs. 3a) corresponding to a_I would be:

$$x = a_I \approx a_{th} \qquad (16)$$

Now combining the concept of a_I (Eq. 16), with Eq. 15:

$$\frac{N\left(\frac{a_{th}}{A}\right)}{N\left(\frac{\infty}{A}\right)} - 1 = (K_t - 1) \exp - (K_t - 1)^{1.5} \left(\frac{a_{th}}{A}\right) \qquad (17)$$

where: $N(a_{th}/A) = [\Delta\sigma(a_{th}/A)\ \Delta\varepsilon(a_{th}/A)\ E]$, stress-strain parameter at the initiated crack length (a_{th}).

A notched specimen subjected to a stress-strain parameter $K_f.\Delta S$ should give the same life as that of a smooth specimen subjected to a stress-strain parameter of $(\Delta\sigma\Delta\varepsilon E)^{\frac{1}{2}}$ (23). Based on this argument, Chen assumed that (23):

$$K_f \cong \frac{N\left(\frac{a_{th}}{A}\right)}{N\left(\frac{\infty}{A}\right)} \qquad (18)$$

The use of Eqs. 17 and 18 lead to Eq. 14:

$$(K_f - 1) = (K_t - 1) \exp - (K_t - 1)^{1.5} \left(\frac{a_{th}}{A}\right) \qquad (14)$$

or

$$q = \frac{K_f - 1}{K_t - 1} = \exp - (K_t - 1)^{1.5} \left(\frac{a_{th}}{A}\right) \qquad (19)$$

From Eq. 14, it can be seen that for a notch of given geometry, K_f would be impossible to evaluate unless a_{th} is known. In this study, Newman's stress intensity correction factor solution (20) has been used (see Section 2.4) which provides accurate values of a_{th}/A and permits the evaluation of K_f.

2.4 Analysis of Failure Lives ($2N_f$)

To obtain K_f (Eq. 14) at a given life requires knowledge of the initiated crack length (a_{th}). In order to solve for K_f at a given life, the Newman's stress-intensity-correction-factor solution (20) and the strain-controlled fatigue concepts (21) are used simultaneously.

At lower stresses, ΔK_{th} determines the initiated crack length ($a_i \simeq a_{th}$, Section 2.3). Newman's stress intensity correction factor solution in an infinite plate with two cracks emanating from an elliptical notch (see Fig. 6a) can be used to describe the threshold condition:

$$\Delta K_{th} = \Delta S[\pi(A + a_{th})]^{\frac{1}{2}} F \tag{20}$$

where: ΔK_{th} = threshold stress intensity factor

ΔS = applied nominal stress range

A = half notch depth

a_{th} = initiated crack length

and F = dimensionless stress intensity correction factor

Equation 20 can be written:

$$\frac{\Delta K_{th}}{[\Delta S(\pi A)^{\frac{1}{2}}]} = F\left[1 + \left(\frac{a_{th}}{A}\right)\right]^{\frac{1}{2}} \tag{21}$$

Figure 6b shows the dimensionless stress intensity correction factor solution as a function of a_{th}/A for different values of K_t. By assuming values of ΔS for a given notch (i.e., K_t and A constant) Fig. 6b may be used to obtain values of a_{th}/A. These a_{th}/A values for a given notch may be used to determine the values of K_f (Eq. 14). The values of ΔS and K_f may be used to obtain the corresponding total life, $2N_f$, since at long lives, the number of reversals to failure, $2N_f$, for R = -1 condition is (19, 21):

$$2N_f = \left[\frac{(K_f \Delta S)}{2\sigma'_f}\right]^{1/b} \tag{22}$$

where: ΔS = applied nominal stress range

K_f = fatigue notch factor

σ'_f = fatigue strength coefficient

and b = fatigue strength exponent

Thus, for a given notch (i.e., A and K_t constant), assuming values of ΔS permits the calculation of associated K_f and $2N_f$ values (Fig. 7). Values of K_f for a selected values of K_t can be found at a chosen life of 10^7 cycles by interpolation (Fig. 8).

3. RESULTS

3.1 General

Knowledge of K_f, K_t and the notch depth (A) permits one to plot $\{(1-q)/q\}$ versus $(1/r)$ at a given life (10^7 cycles) and thus, to study the notch size effect: see Fig. 1b and Eq. 19. Equation 19 predicts that q is a function of both K_t and A, thus, is apparently not a unique function of r. One has, therefore, two choices in experimentally or analytically studying the notch size effect: the notch size effect can be studied

(i) as a function of r, holding K_t (Eq. 8) or A/r constant, i.e., geometrically similar notches (Fig. 9),

or

(ii) as a function of r (for elliptical notches) holding the notch depth (A) constant, i.e., for different values of K_t (Eq. 8) or A/r (Fig. 10).

Generally, these above points regarding the notch size effect have been neither appreciated nor adequately described in the literature. Figure 9 shows the influence of K_t on the notch size effect, and Fig. 10 shows rather different behavior which would result from holding the notch depth (A) constant.

3.2 Comparison of Predictions with Experimental Results Reported in the Literature

To assess the validity of the analytical model for K_f (Eq. 14) and q (Eq. 19), the studies of the notch size effect by NASA (4) and Frost (24) were compared with the predictions based on the proposed analytical model. Since notch size effect studies seldom report strain-controlled fatigue properties of the materials studied, the properties used in these

comparisons (steel and aluminum alloys) have been taken from the literature (see Table 1). All predictions assume an infinite plate and use Eqs. 14, 21, 22 and Fig 6b for elliptical notches under axial loading (R = -1 condition) to generate K_f versus $2N_f$ (Fig. 8) as a function of K_t (K_t = 3, 5 and 9).

Data on experimental studies of the notch-size effect for aluminum alloy specimens have been collected by Kuhn et. al (4). Data from tests in which K_t is held constant is compared with the predictions of the analytical model in Fig. 11. Also, data from studies based on fixed notch depths (A) are compared with the predictions of the analytical model in Figs. 12-13. It should be noted that the predictions based on A of 0.2 in. for 7075-T6 aluminum alloy (Fig. 13) have been compared with the U-notched aluminum alloy based on A of 0.22 in. and 0.375 in. It is expected that the predictions based on A of 0.375 in. would not differ very much from the predictions based on A of 0.2 in. (see Fig. 10).

Frost (24) studied the effects of the notch root radius (r) on the fatigue strength of notched specimens in a series of carefully performed experiments. Mild steel (24) V-notched specimens were prepared having various notch root radii but a constant notch depth (A = 0.2 in.). After having the notches machined in them, the mild steel specimens were annealed to relieve the stresses introduced by machining. A comparison of Frost's data for mild steel and predictions using the mechanical properties of A-36 steel is given in Fig. 14.

The experimental results shown in Figs. 11-14 are in generally good agreement with the predictions which gives confidence in the validity of the proposed analytical model. Also, the results of the present study

suggests that the behavior of the materials studied is best represented by Peterson's equation, since a striking feature of Figs. 9-14 is that for both the elliptical notches and the geometrically similar notches, the resultant values of the exponent (B) in Eq. 5 are 0.8 or larger, that is, very close to the exponent of one of Peterson's equation (Eq. 11) rather than the exponent of one-half of Neuber's equation (Eq. 9).

3.3 Other Phenomena Related to the Notch-Size Effect

Two phenomena associated with the notch-size effect have been predicted using the developed analytical model: (a) the variation of K_f with K_t and (b) the formation of nonpropagating cracks. The following sections give the predictions of the model and the verifications of these predictions using the experimental results of Frost (24, 25).

3.3.1 Relationship between K_f and K_t

Plots of the variation of K_f as a function of K_t (see Fig. 15) developed by Frost (25) offer a convenient way to view the notch-size effect for elliptical notches. The predicted variation of K_f with K_t for A-36 steel (24) and 2014-T6 aluminum alloy (25) is shown in Figs. 16 and 17. Also plotted in Fig. 16 are the experimental results of Frost for mild steel (24). Frost's experimental results for round bar specimens of BS L65 aluminum alloy (25) (assumed to be equivalent to 2014-T6 aluminum alloy) have been plotted in Fig. 17. No such data for plate specimens are available. The predictions of the analytical model show good agreement with the experimental results (Figs. 16 - 17).

Figures 15-17 confirm the notion of $K_{f,max}$, a useful concept for predicting the fatigue strength of notched component with a wide or unknown

range of notch root radii, e.g., weldments; since in these figures K_f achieves a maximum value at a certain value of K_t.

3.3.2 Nonpropagating Cracks

The occurance of nonpropagating fatigue cracks has been explained by Frost (24) in terms of a stress (S) versus K_t plot, see Fig. 18 (24-26). Such S - K_t plots (Fig. 18) can be generated using the analytical model developed:

$$S_n = \frac{S_a}{K_f} \tag{23}$$

S_n = fatigue strength of notched specimen at a given life

and

S_a = fatigue strength of smooth specimen at a given life

S_n represents the minimum stress that is necessary to cause complete fatigue fracture. At any stress (S) above S_n would lead to complete fatigue fracture. S_n (line 1 in Fig. 18) is a function of the notch depth (A) (see Fig. 19) since K_f is a function of A (Fig. 15).

The minimum stress (S_i) that would cause fatigue cracks to initiate at the notch root can be estimated by replacing S_n and K_f in Eq. 23 by S_i and K_t:

$$S_i = \frac{S_a}{K_t} \tag{24}$$

Thus, S_i (line 3 in Fig. 18) represents the stress below which no cracks can be present but above which cracks should be present at the notch root.

The predicted variations of S_i and S_n versus K_t for A-36 steel and 2014-T6 aluminum alloy are shown in Figs. 20 and 21. Also plotted in Figs. 20 and 21 are the results for mild steel (24), similar to A-36 steel, and

BS L65 aluminum alloy (25) equivalent to 2014-T6 aluminum alloy. Predictions for mild steel (Fig. 20) show better agreement than those of the aluminum alloy (Fig. 21) possibly because of a difference between the material properties assumed in the predictions and the actual properties of the material studied in the experimental work.

Thus, at any stress, $S_n > S > S_i$ (Figs. 18-21), fatigue cracks will initiate, grow and become dormant unless the stress level (S) is raised to S_n which represents the minimum stress necessary to cause fatigue crack propagation to final fracture.

Nonpropagating cracks can be present in notched specimens having K_t exceeding some critical value (see K_{t_c}, in Fig. 18). Such critical K_t values increase, and the regions over which the nonpropagating cracks can be present (bounded by S_i and S_n, Fig. 18) decrease with increasing A (see Fig. 19). The influence of the material properties on the formation of the nonpropagating cracks is shown in Fig. 22. To make such comparisons, the variations of S_n and S_i as a function of K_t have been predicted for A-36 steel and HY-130 steel for notches having A equal to 0.2 in. HY-130 steel (a high strength quenched and tempered steel) requires a sharper notch (higher K_t) in order to initiate nonpropagating cracks at the notch root than does the A-36 steel (a mild, lower strength steel) (Fig. 22).

The length of nonpropagating cracks and the dependence on the stress level of this length on (S) may be predicted by rearranging Eq. 15 as follows:

$$x = -\frac{A}{(K_t - 1)^{1.5}} \ln \frac{\frac{N(x/A)}{N(\infty/A)} - 1}{K_t - 1} \qquad (25)$$

For elastic condition, Eq. 25 may be written as:

$$x = - \frac{A}{(K_t - 1)^{1.5}} \ell n \frac{\frac{\sigma(x/A)}{S} - 1}{K_t - 1} \quad (26)$$

where

$\sigma(x/A)$ = local stress amplitude ahead of a notch-root as a function of the distance (x)

and

S = applied nominal stress amplitude

It has been shown that the nonpropagating crack of length (x) can penetrate into the material from the notch root provided the local stress level is higher than the fatigue strength of the smooth specimen (27). Using this argument and replacing $\sigma(x/A)$ by S_a, Equation 26 may be written as:

$$x = - \frac{A}{(K_t - 1)^{1.5}} \ell n \frac{\frac{Sa}{S} - 1}{K_t - 1} \quad (27)$$

It may be seen from Eq. 27 that the length of the nonpropagating crack is not only dependent on S but is also dependent on A and K_t. The predicted variation of the nonpropagating crack as a function of S/S_a (for K_t = 8.3, and 14 with A = 0.2 in.) has been shown in Fig. 23 together with the experimental results (17, 27) for mild steel and aluminum alloys. The agreement between the predictions and the experimental results seems to be good (Fig 23).

4. DISCUSSION

4.1 Effect of the Material Properties on the Notch Sensitivity Index (q)

An interesting feature of the proposed analytical model is that the effect of the material property variations (ΔK_{th}, σ_f', b) on the notch sensitivity index (q) can be predicted (Eqs. 14, 21 and 22). The influence of ΔK_{th} on q for 2014-T6 aluminum alloy (other properties constant) is shown in Fig. 24. It can be seen from Fig. 24 that the materials with lower ΔK_{th} values are more sensitive to the effects of the notches. The influence of the strain-controlled fatigue properties is illustrated in Fig. 25 which shows the predicted variation of $\{(1 - q)/q\}$ as a function of (1/r) for 7075-T6 aluminum alloy with two different sets of properties (σ_f' and b) reported in the literature. The material with higher long-life fatigue resistance should be more sensitive to the effects of notches (Fig. 25).

4.2 Material Constant (a)

The influence of notch depth (A) on the material constant (a) is shown in Fig. 26 for different steels and aluminum alloys containing elliptical notches (that is notches for which K_t is given by Equation 8). The predictions of (a) shown in this figure have been made for notches with values of A from 0.008 to 1 in. which is the range of practical interest. For a given material, (a) increases with decreasing A (Fig. 26) resulting in a decreased susceptibility of a material to notches of given notch-root radius (r) with shallower notches depths (A). Although not very great, the influence of A on (a) is greatest for A-36 steel for notches deeper than 0.2 in.

Using the proposed analytical model, values of (a) for elliptically notched specimens having A equal to 0.2 in. have been predicted for steels and aluminum alloys. The predicted values of (a) may be fitted by a simple equation when plotted as a function of $\Delta K_{th}/S_a$ (solid line in Fig. 27). The best fit line (solid line, Fig. 27) is:

$$a = 0.18 \left[\frac{\Delta K_{th}}{S_a}\right]^{2.27} \tag{28}$$

A dimensionally correct (or at least more convenient) relationship also shown (dashed line in Fig. 27) is:

$$a \cong 0.14 \left[\frac{\Delta K_{th}}{S_a}\right]^{2} \text{ in.} \tag{29}$$

Independently determined experimental values of (a), ΔK_{th} and S_a were taken from the literature (see Table 2) and plotted in Fig. 27 in order to compare the predicted variation of (a) as a function of $\Delta K_{th}/S_a$ with the data of entirely experimental origin. Except for mild steel (24) and BS L65 aluminum alloy (25), it is not known whether (a) for other materials were determined with notches having a depth of 0.2 in. The predictions agree well with the experimental results.

Values of (a) for steels based on assumed strain-controlled fatigue properties estimated from S_u(28) and an assumed constant value of ΔK_{th} = 10 ksi $(\text{in.})^{1/2}$ have been predicted and are shown in Fig. 28 as a function of S_u. The predicted (a) values show good agreement with values of (a) (see Fig. 28)estimated using Equation 4:

$$a = 0.001 \left[\frac{300}{S_u}\right]^{1.8} \text{ in.} \tag{4}$$

4.3 Extrapolation of the Notched Specimen Concepts to Specimens Containing Cracks

Use of linear elastic fracture mechanics (LEFM) to predict the fatigue strength of small cracks has been questioned because LEFM predicts lower crack growth rates and much higher threshold stresses than are actually exhibited by "short cracks" (29-32). An attempt has been made to predict the fatigue strength of cracked specimens containing both long and short cracks using Peterson's equation (Eq. 11). To make such predictions, a specimen containing a sharp crack has been assumed to be equivalent to a specimen containing a notch of the same length but as suggested by Jack et. al (33) with a notch root radius (r) equal to a critical value (r_c) at which the fatigue strength of cracked and notched specimens are identical.

This analysis considers elliptical notches in an infinite plate and assumes the validity of Peterson's equation (Eq. 11); since as shown in Section 3.2, Peterson's equation correctly represents the notch-size effect behavior of the materials studied. Equation 11 may be written:

$$\frac{S_a}{S_n} = 1 + \frac{2\sqrt{A/r}}{1 + a/r} \tag{30}$$

since

$$K_f = \frac{S_a}{S_n} \text{ (definition)} \tag{31}$$

or

$$\frac{S_n}{S_a} = \frac{1 + a/r}{1 + \frac{a}{r} + 2\sqrt{A/r}} \tag{32}$$

It is known that largest value of K_f ($K_{f,max}$) results when r is equal to (a) (Equations 12 and 13). Jack et. al (33) also showed that for mild steel, a cracked specimen would give a fatigue strength similar to a notched specimen having the same notch depth but with a root radius (r) equal to 0.01

in. This value of root radius (r) is roughly equal to the material constant (a) for mild steel. Thus, assuming r in Equation 32 is equal to (a), Equation 32 becomes:

$$\left.\frac{S_n}{S_a}\right|_{r_c = a} = \frac{1}{1 + (A/a)^{\frac{1}{2}}} \tag{33}$$

The interesting aspects of Equation 33 are that:

(i) fatigue strength of the cracked specimens containing both long and short cracks can be well represented by an analysis for elliptical notches in an infinite plate, and

(ii) an universal plot such as Fig. 29 can be made if S_n/S_a is plotted as a function of A/a on log-log scale.

Figure 29 shows the comparisons between the predictions using Equation 33 and the experimental results for edge cracked specimens of mild steel (24) equivalent to A-36 steel and BS L65 aluminum alloy (34) assuming crack length (ℓ) to be equivalent to notch depth (A). For such comparisons, the crack length (ℓ) of mild steel (24) and BS L65 aluminum alloy (34) have been normalized by their respective values of (a) corresponding to a fixed notch depth of 0.2 in. The predictions in general agree well with the experimental results (see Fig. 29).

4.4 Relationship of ℓ_o From the Work of Haddad (30, 31) with the Material Constant (a)

Haddad et. al (30, 31) studied the behavior of "short cracks" using LEFM. Starting with the definition of threshold stress intensity factor (ΔK_{th}):

$$\Delta K_{th} = \Delta S_c \, (\pi \ell)^{\frac{1}{2}} \tag{34}$$

where

ΔS_c = range of fatigue strength for cracked specimen

or

$$\frac{\Delta S_c}{\Delta S_a} = \frac{S_c}{S_a} = \frac{\Delta K_{th}}{\Delta S_a}\left[\frac{1}{\pi \ell}\right]^{\frac{1}{2}} \tag{35}$$

The predicted variation of $\frac{S_c}{S_a}$ versus ℓ using Equation 35 is shown in Figure 30. Since the LEFM approach could not properly predict fatigue strength of cracked specimen in the "shorter crack" regions. Haddad et. al (30, 31) modified the LEFM approach (Equations 34 and 35) by introducing an intrinsic crack length (ℓ_o) which they postulated to be a material constant. They evaluated ℓ_o by setting Equation 35 to one (see Figure 30):

$$\frac{S_c}{S_a} = \frac{\Delta K_{th}}{\Delta S_a}\left[\frac{1}{\pi \ell}\right]^{\frac{1}{2}} = 1 \tag{36}$$

or

$$\ell_o = \ell = \frac{1}{\pi}\left[\frac{\Delta K_{th}}{\Delta S_a}\right]^{\frac{1}{2}} \tag{37}$$

Subsequently, the modified form of Equation 35 suggested by Haddad et al. is:

$$\frac{S_c}{S_a} = \frac{\Delta K_{th}}{\Delta S_a}\left[\frac{1}{\pi(\ell+\ell_o)}\right]^{\frac{1}{2}} \tag{38}$$

The predicted variation of $\frac{S_c}{S_a}$ as a function of ℓ using Equation 38 is shown in Figure 30.

Using the relationship of Equation 37, Equation 38 may also be written as:

$$\frac{S_c}{S_a} = \frac{1}{(1 + \ell/\ell_o)^{\frac{1}{2}}} \tag{39}$$

Tanaka et. al (50) showed that a plot of $\frac{S_c}{S_a}$ versus ℓ/ℓ_o should give an universal plot (see Figure 31). It has been proposed in Section 4.3 that a plot of $\frac{S_n}{S_a}$ versus A/a based on notched specimen behavior (Equation 33) also could represent the data for cracked specimens. It can, however, be seen that Equations 33 and 39 are not identical (see Figure 31) although quite similar.

The relationship between (a) and $(\Delta K_{th}/S_a)$ (Equation 29) which was developed in Section 4.2 permits us to evaluate ℓ_o in terms of the material constant (a). Recalling Equation 29:

$$a = 0.14\left(\frac{\Delta K_{th}}{S_a}\right)^2 \text{ in.} \tag{29}$$

or

$$\Delta K_{th} = 0.75\ \Delta S_a(\pi a)^{\frac{1}{2}} \text{ ksi } (\text{in.})^{\frac{1}{2}} \tag{40}$$

For a cracked specimen containing a crack of length (2ℓ)

$$\Delta K_{th} = F.\Delta S_c\ (\pi\ell)^{\frac{1}{2}} \text{ ksi } (\text{in.})^{\frac{1}{2}} \tag{41}$$

where

F = correction factor depending on the geometry of the crack.

Thus, using Equation 41, Equation 40 may be written:

$$\frac{\Delta S_c}{\Delta S_a} = \frac{S_c}{S_a} = \frac{0.75}{F}\ (a/\ell)^{\frac{1}{2}} \tag{42}$$

The value of ℓ_o (proposed by Haddad et. al) can be evaluated in terms of (a) by setting Equation 42 to one $(\ell=\ell_o)$:

$$\frac{S_c}{S_a} = \frac{0.75}{F}\ (a/\ell)^{\frac{1}{2}} = 1 \tag{43}$$

or

$$\ell o = \frac{0.56a}{F^2} \text{ in.} \tag{44}$$

It is seen from Equation 44 that ℓ_o is related to (a) and the geometry of the crack (F). For an edge cracked specimen:

$$\ell_o = 0.45\ a \text{ in.} \tag{45}$$

For a center cracked specimen:

$$\ell_o = 0.56\ a \text{ in.} \tag{46}$$

While, for a semicircular surface crack:

$$\ell_o \simeq a \text{ in.} \tag{47}$$

Figure 32 shows a comparison between the predicted ℓ_o (computed using Equation 44) and the experimentally obtained ℓ_o. With the exception of Frost's data for which all necessary data was reported, comparisons with ℓ_o have been calculated from the ultimate tensile strength (S_u) and Equations 4 and 44. The predicted ℓ_o show good agreement with experimentally determined ℓ_o (Figure 32).

5. OBSERVATIONS AND CONCLUSIONS

The results based on the analytical model proposed herein considered elliptical notches in an infinite plate subjected to completely reversed axial stress at a life of 10^7 cycles and led to the following observations and conclusions:

(1) Using a simple relationship for K_f as a function of K_t and the initiated crack length (a_I), it has been shown that the fatigue notch sensitivity index (q), for a given material, depends on K_t for geometrically similar notches and on notch depth (A) for elliptical notches. The predictions using this analytical model showed good agreement when compared with the Frost's experimental results and the NASA's collected experimental results on the notch-size effect.

(2) This study leads one to conclude that the fatigue behavior of the notched materials is better represented by Peterson's equation (Eq. 3) than by Neuber's equation (Eq. 2), particularly when K_t is based on perfect elasticity. The proposed analytical model, therefore, appears to lend strong support to the concept of using the $K_{f,max}$ condition for elliptical notches.

(3) Based on Peterson's equation (Eq. 3), a general relationship for the material parameter (a) (often considered to be a material constant), has been established as a function of the strain-controlled fatigue properties and the crack propagation constant, ΔK_{th}. This relationship seems to apply to both steels and aluminum alloys. The significant feature of such a correlation is that it overcomes the long standing problem regarding the values of the material parameter (a) for aluminum alloys.

(4) The analytical model developed for K_f has been used successfully to study the condition for the formation of the nonpropagating cracks. The maximum length of the nonpropagating cracks that can be present at the root of a notch has been evaluated.

(5) An universal plot of (S_n/S_a) versus (A/a) based on elliptical notches has been proposed which has been used successfully to represent the fatigue strength of cracked specimens.

(6) The intrinsic crack length (ℓ_o) as proposed by Haddad et. al was related to the material constant (a).

REFERENCES

1. Forsyth, P. J. E., "The Physical Basis of Metal Fatigue," American Elsevier Publishing Co., Inc., New York, 1969.

2. Neuber, H., "Theory of Notch Stresses: Principle for Exact Stress Calculations," J. W. Edwards, Ann Arbor, Michigan, 1946.

3. Kuhn, P. and Hardrath, H. F., "An Engineering Method for Estimating Notch-Size Effect in Fatigue Tests on Steels," National Advisory Committee for Aeronautics, Technical Note 2805, Oct., 1952.

4. Kuhn, P. and Figge, I. E., "Unified Notch-Strength Analysis for Wrought Aluminum Alloys," National Aeronautics and Space Administration, Technical Note D-1259, May, 1962.

5. Peterson, R. E., "Notch-Sensitivity," Metal Fatigue, Chap. 13, Sines and Waisman, Editors, McGraw-Hill Book Co., Inc., 1959.

6. Peterson, R. E., "Analytical Approach to Stress Concentration Effect in Fatigue of Aircraft Materials," Proceedings on Fatigue of Aircraft Structures, WADC Technical Report No. 59-507, August, 1959, pp. 273-299.

7. Aphanasiev, N. N., "The Effect of Shape and Size Factors on the Fatigue Strength," The Engineers' Digest, Vol. 5, No. 3, March-April, 1948, pp. 132-136.

8. Heywood, R. B., "Design by Photoelasticity," Chapman and Hall Ltd., London, 1952, p. 348.

9. Harris, W. J., "Size Effects and Their Possible Significance for Non-propagating Cracks in Metal," Metallurgia, Vol. 57, No. 342, April, 1958, pp. 193-197.

10. Endo, K. and Uede, T., "Studies on the Size Effect of Bending and Twisting Fatigue Strength," Bulletin, Japanese Society of Mechanical Engineers, Vol. 8, No. 31, August, 1965, pp. 314-321.

11. Kuguel, R., "A Relation between Theoretical Stress Concentration Factors and Fatigue Notch Factor Deducted from the Concept of Highly Stressed Volume," Proceedings, American Society for Testing and Materials, Vol. 61, 1961, pp. 732-748.

12. Switek, W. and Buch, A., "The Problem of Maximum Notch Effect in Case of Flat Elements with Transverse Holes," Proceedings of the Third Conference on Dimensioning and Strength Calculations, Hungarian Academy of Science, Budapest, Nov., 1968, pp. 275-286.

13. Raske, D. T., "Fatigue Failure Predictions for Plates with Holes and Edge Notches," Journal of Testing and Evaluation, Vol. 1, No. 5, Sept., 1973, pp. 394-404.

14. Raske, D. T., "The Variation of the Fatigue Notch Factor with Life," M. S. Thesis, University of Illinois at Urbana-Champaign, Illinois, 1971.

15. Raske, D. T., "Section and Notch Size Effects in Fatigue," T.&A.M. Report No. 360, Department of Theoretical and Applied Mechanics, University of Illinois, Urbana, IL, August, 1972.

16. Yen, C. S. and Dolan, T. J., "A Critical Review of the Criteria for Notch-Sensitivity in Fatigue of Metals," University of Illinois Bulletin, Vol. 49, No. 53, March, 1952.

17. Frost, N. E. and Dugdale, D. S., "Fatigue Tests on Notched Mild Steel Plates with Measurements of Fatigue Cracks," Journal of Mechanics and Physics of Solids, Vol. 5, 1957, pp. 182-192.

18. Morrow, JoDean, "Fatigue Properties of Metals," SAE Fatigue Design Handbook, Section 3.2, Graham, J. A., Editor, Society of Automotive Engineers, 1968, pp. 21-30.

19. Higashida, Y. and Lawrence, F. V., "Strain Controlled Fatigue Behavior of Weld Metal and Heat-Affected Base Metal in A-36 and A514 Steel Welds," FCP Report No. 22, College of Engineering, University of Illinois, Urbana, August, 1976.

20. Newman, J. C., Jr., "An Improved Method of Collocation for the Stress Analysis of Cracked Plates with Various Shaped Boundaries," NASA TN D-6376, 1971.

21. Morrow, JoDean, "Cyclic Plastic Strain Energy and Fatigue of Metals," ASTM STP 378, American Society for Testing and Materials, 1965, pp. 45-87.

22. Socie, D. F., Morrow, JoDean and Chen, W. C., "A Procedure for Estimating the Total Fatigue Life of Notched and Cracked Members," Journal of Engineering Fracture Mechanics, Vol. 11, No. 4, 1979, pp. 851-860.

23. Chen, W. C. and Lawrence, F. V., "A Model for Joining the Fatigue Crack Initiation and Propagation Analysis," FCP Report No. 32, College of Engineering, University of Illinois, Urbana, November, 1979.

24. Frost, N. E. "A Relation between the Critical Alternating Propagation Stress and Crack Length for Mild Steel," Proceedings Institutions of Mechanical Engineers, Vol. 173, No. 35, 1959, pp. 811-836.

25. Frost, N. E., "Nonpropagating Cracks in V-Notched Specimens Subject to Fatigue Loading," The Aeronautical Quarterly, Vol. 8, 1957, pp. 1-20.

26. Fenner, A. J., Owne, N. B. and Phillips, C. E., "Fatigue Crack as a Stress-Raiser," Engineering, Vol. 171, 1951, pp. 637.

27. Frost, N. E., "Crack Formation and Stress Concentration Effects in Direct Stress Fatigue," Engineer, Vol. 200, 1955, pp. 464-467 and 501-503.

28. Socie, D. F., Mitchell, M. R. and Caulfield, E. M., "Fundamental of Modern Fatigue Analysis," FCP Report No. 26, College of Engineering, University of Illinois, Urbana, IL, April, 1977.

29. Pearson, S., "Initiation of Fatigue Cracks in Commercial Aluminum Alloys and the Subsequent Propagation of Very Short Cracks," Engineering Fracture Mechanics, Vol. 7, 1975, pp. 235-247.

30. Haddad, M. H. El., Topper, T. H. and Smith, K. N., "Prediction of Non-propagating Cracks," Engineering Fracture Mechanics, Vol. 11, 1979, pp. 573-584.

31. Haddad, M. H., Smith, K. N. and Topper, T. H., "Fatigue Crack Propagation of Short Cracks," Journal of Engineering Materials and Technology, Trans. ASME, Vol. 101, 1979, pp. 42-46.

32 Talug, A. and Reifsnider, K., "Analysis and Investigation of Small Flaws," ASTM STP 637, American Society for Testing and Materials, 1977, pp. 81-96.

33. Jack. A. R. and Price, A. T., "The Initiation of Fatigue Cracks from Notches in Mild Steel Plates," International Journal of Fracture Mechanics, Vol. 6, No. 4, 1970, pp. 401-409.

34. Frost, N. E., "Notch Effects and the Critical Alternating Stress Required to Propagate a Crack in an Aluminum Alloy Subject to Fatigue Loading," Journal of Mechanical Engineering Science, Vol. 2, No. 2, 1960, pp. 109-119.

35. Majumdar, S. and Morrow, JoDean, "Correlation between Fatigue Crack Propagation and Low Cycle Fatigue Properties," ASTM STP 559, American Society for Testing and Materials, 1974, pp. 159-182.

36. Majumdar, Surindranath, "Low Cycle Fatigue Behavior and Crack Propagation in Some Steels," T.&A.M. Report No. 387, Department of Theoretical and Applied Mechanics, University of Illinois, Urbana, IL, 1974.

37. Ford Motor Co., "Monotonic and Cyclic Properties of Engineering Materials," June, 1972.

38. Nordmark, G. E., Private Communication, Alcoa Research Labs., Alcoa, PA, 1980.

39. Davenport, R. T. and Brook, R., "The Threshold Stress Intensity Range in Fatigue," Fatigue of Engineering Materials and Structures, Vol. 1, 1979, pp. 151-158.

40. Grover, H. J. and Hyler, W. S., "Axial-Load Fatigue Properties of 24S-T and 75S-T Aluminum Alloy as Determined in Several Laboratories," NACA TN 2928, May, 1953.

41. Hertzberg, R. W., "Deformation and Fracture Mechanics of Engineering Materials," John Wiley and Sons, 1976.

42. Mattos, R. J. and Lawrence, F. V., "Estimation of the Fatigue Crack Initiation Life in Welds Using Low Cycle Fatigue Concepts," FCP Report No. 19, College of Engineering, University of Illinois, Urbana, IL, October, 1975.

43. Rolfe, S. T. and Barsom, J. M., "Fracture and Fatigue Control in Structures - Applications of Fracture Mechanics, Prentice-Hall, Inc., NJ, 1977.

44. Usami, S. and Shida, S., "Elastic-Plastic Analysis of the Fatigue Limit for a Material with Small Flaws," Fatigue of Engineering Materials and Structures, Vol. 1, 1979, pp. 471-481.

45. Socie, D. F., "Prediction of Fatigue Crack Growth in Notched Members under Variable Amplitude Loading History," Engineering Fracture Mechanics, Vol. 9, No. 4, 1977, pp. 849-865.

46. Kurath, P., Private Communication, Department of Theoretical and Applied Mechanics, University of Illinois, Urbana, IL, 1980.

47. Streicher, E., Private Communication, Department of Metallurgy and Mining Engineering, University of Illinois, Urbana, IL, 1980.

48. Frost, N. E., Marsh, K. J. and Pook, L. P., "Metal Fatigue," Clarendon Press, Oxford, 1974.

49. Hudson, C. M., "Effect of Stress Ratio on Fatigue Crack Growth in 7075-T6 and 2024-T3 Aluminum Alloy Specimens," National Aeronautics and Space Administration, Technical Note D-5390, August, 1969.

50. Tanaka, K., Nakai, Y. and Yamashita, M., "Fatigue Growth Threshold of Small Cracks," Private Communication, Department of Engineering Science, Kyoto University, Kyoto, Japan, 1980.

TABLE 1

MATERIAL PROPERTIES

	Monotonic Properties					Cyclic Properties				
Steel	Young's Modulus E ksi	Yield Strength* S_y ksi	Ultimate Tensile Strength S_u ksi	True Fracture Strength σ_f ksi	True Fracture Ductility ε_f	Cyclic Strain Hardening Exponent n'	Fatigue Strength Coefficient σ_f' ksi	Fatigue Strength Exponent b	Threshold Stress Intensity Factor ΔK_{th} (at R = -1) ksi $(in)^{\frac{1}{2}}$	Ref.
A-36	27.5×10^3	36	75	---	---	0.14	125	-0.085	11	30, 35
HY-130	28.0×10^3	147	160	224	0.92	0.100	216	-0.060	5.5†	23, 36
2014-T6	10.0×10^3	67	74	---	0.29	0.16	123	-0.106	2.75†	37, 38
2024-T3	10.6×10^3	55	68	---	0.28	0.065	160	-0.124	3.8	37, 49
7075-T651	10.1×10^3	77.9	85.4	95.1	0.145	0.04	241.4	-0.149	2.5†	23
7075-T6	10.3×10^3	68	84	108	0.41	0.146	278.1	-0.176	3.5	23, 41
7075-T6	10.3×10^3	68	84	108	0.41	0.146	191	-0.126	3.5	37, 41

*0.2% offset

†Represent ΔK_{th} values at R = 0 condition. ΔK_{th} values at R = -1 condition have been calculated from ΔK_{th} values at R = 0 condition using $\Delta k_{th} = (1 - R)\ \Delta K_{th(o)}$ (39).

TABLE 2

EXPERIMENTAL VALUES OF MATERIAL CONSTANT (a), FATIGUE LIMIT (S_a) AND THRESHOLD STRESS INTENSITY FACTOR (ΔK_{th})

Material	$S_{a(10^7)}$ ksi	ΔK_{th} ksi $(in)^{\frac{1}{2}}$	a in.	Ref.
Mild steel	32	11	0.013	24, 30
BS L65	22	3.48	0.00313	25, 31
7075-T6	15 - 27.5	3.5	0.003	6, 40, 41
A-36	31	11	0.018	18, 30, 42
HY-130	55	10	0.0031	18, 23, 43
2024-T3	17 - 23	3.8	0.008	6, 4, 49

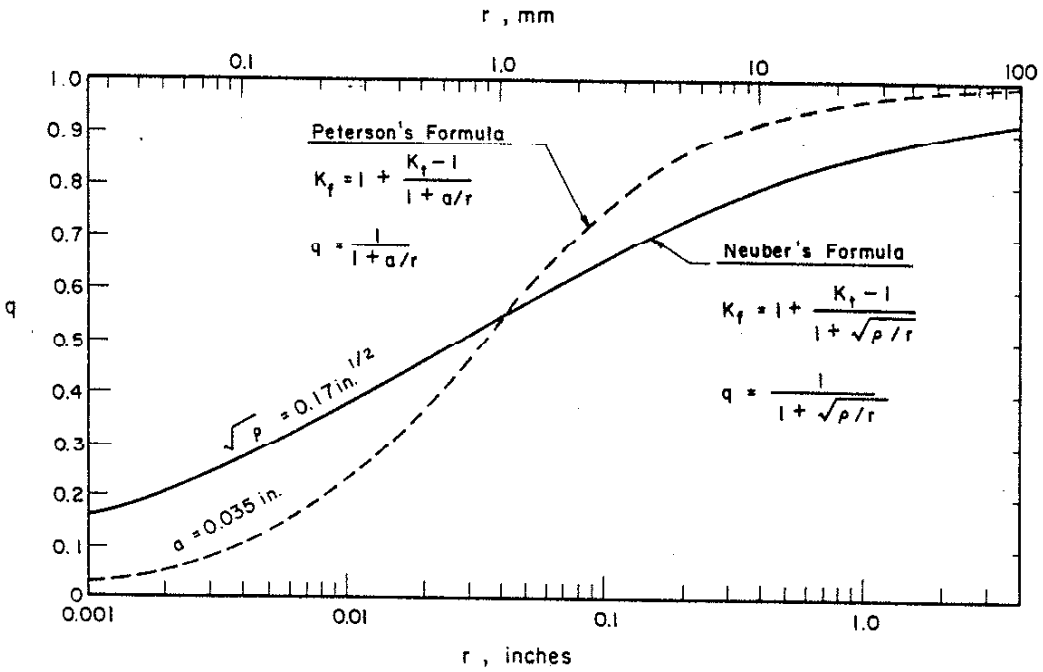

(a)

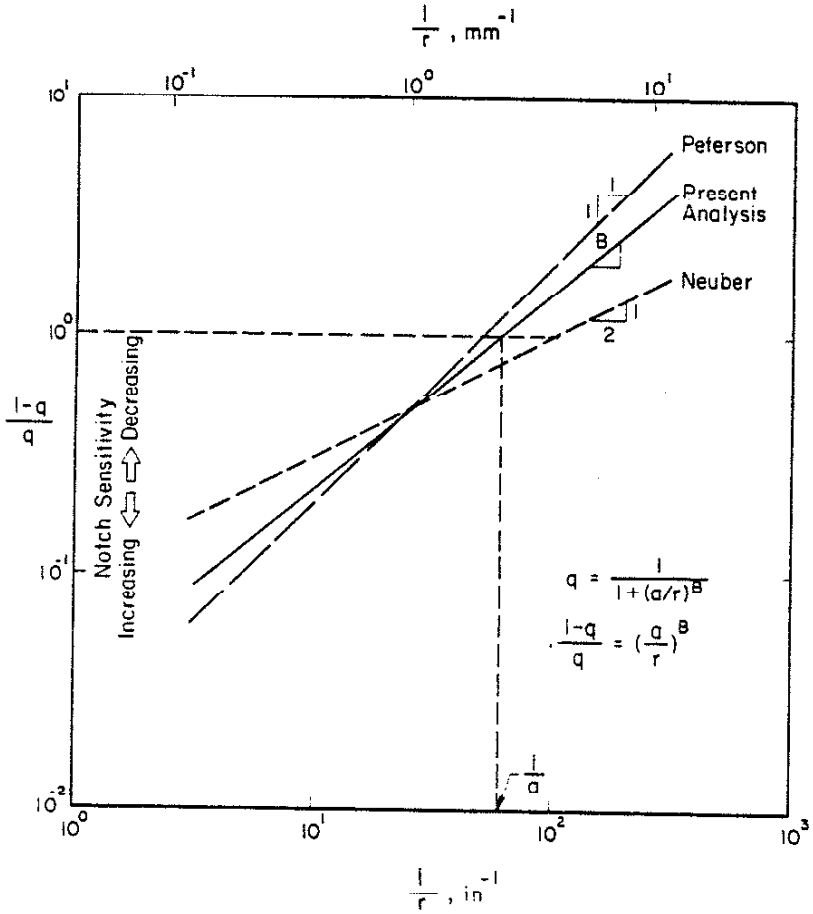

(b)

FIG. 1 EVALUATION OF THE NOTCH SIZE EFFECT USING q-log r AND log{(1 - q)/q} - log(1/r) PLOT

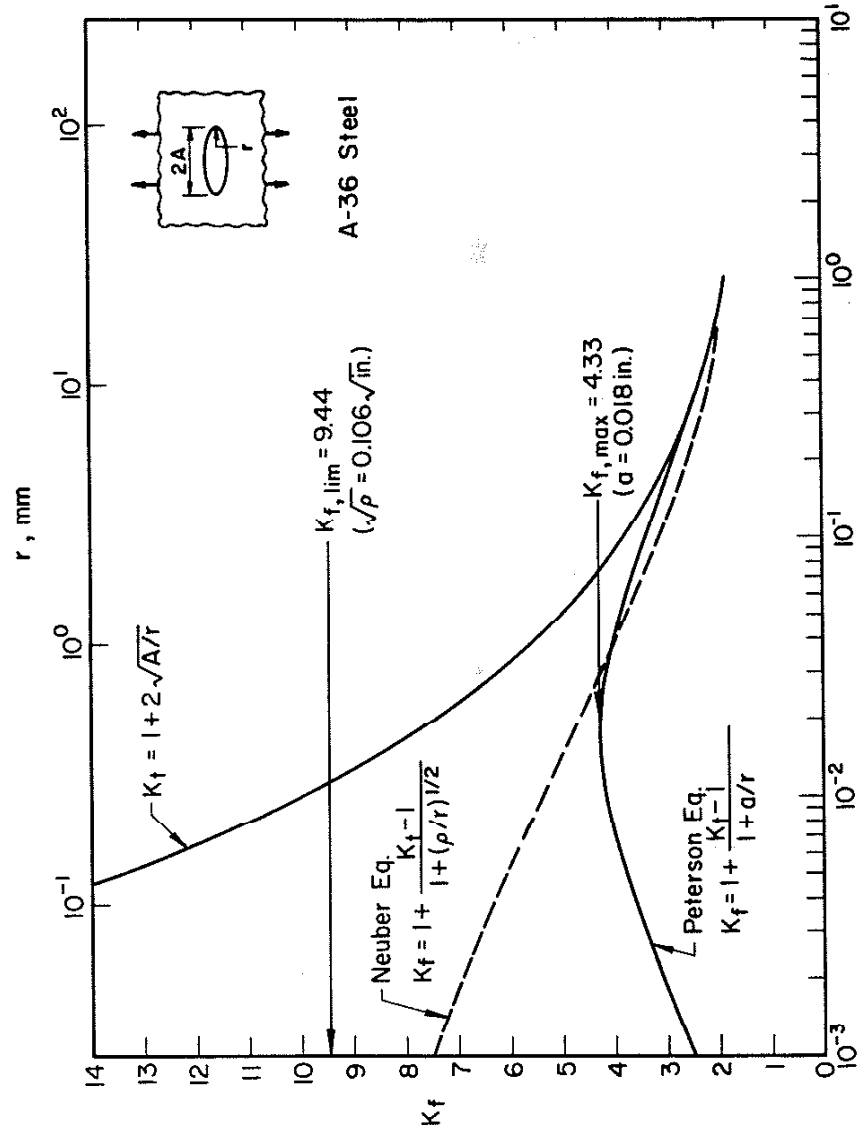

FIG. 2 MAXIMUM VALUES OF K_f($K_{f,lim}$ AND $K_{f,max}$) BASED ON NEUBER AND PETERSON EQUATIONS FOR A-36 STEEL

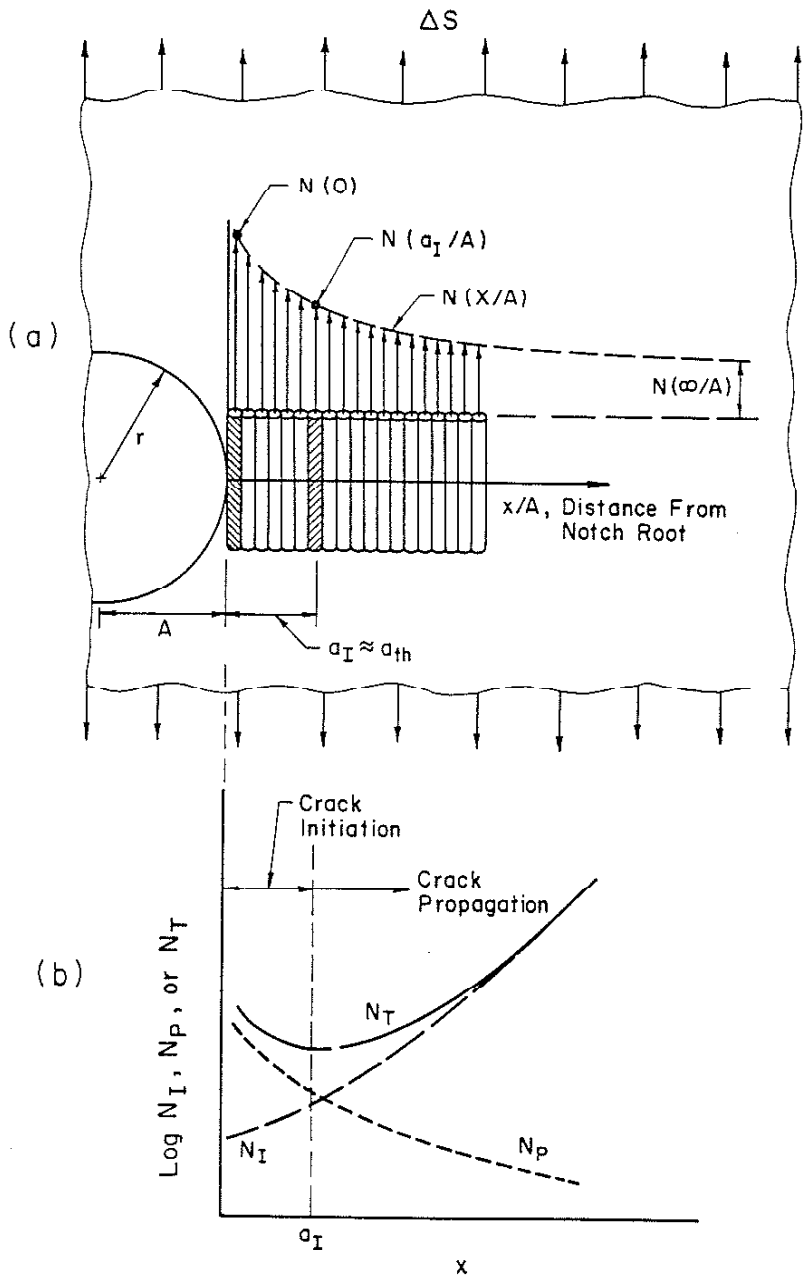

FIG. 3 CHEN'S DEFINITION OF a_I (23)

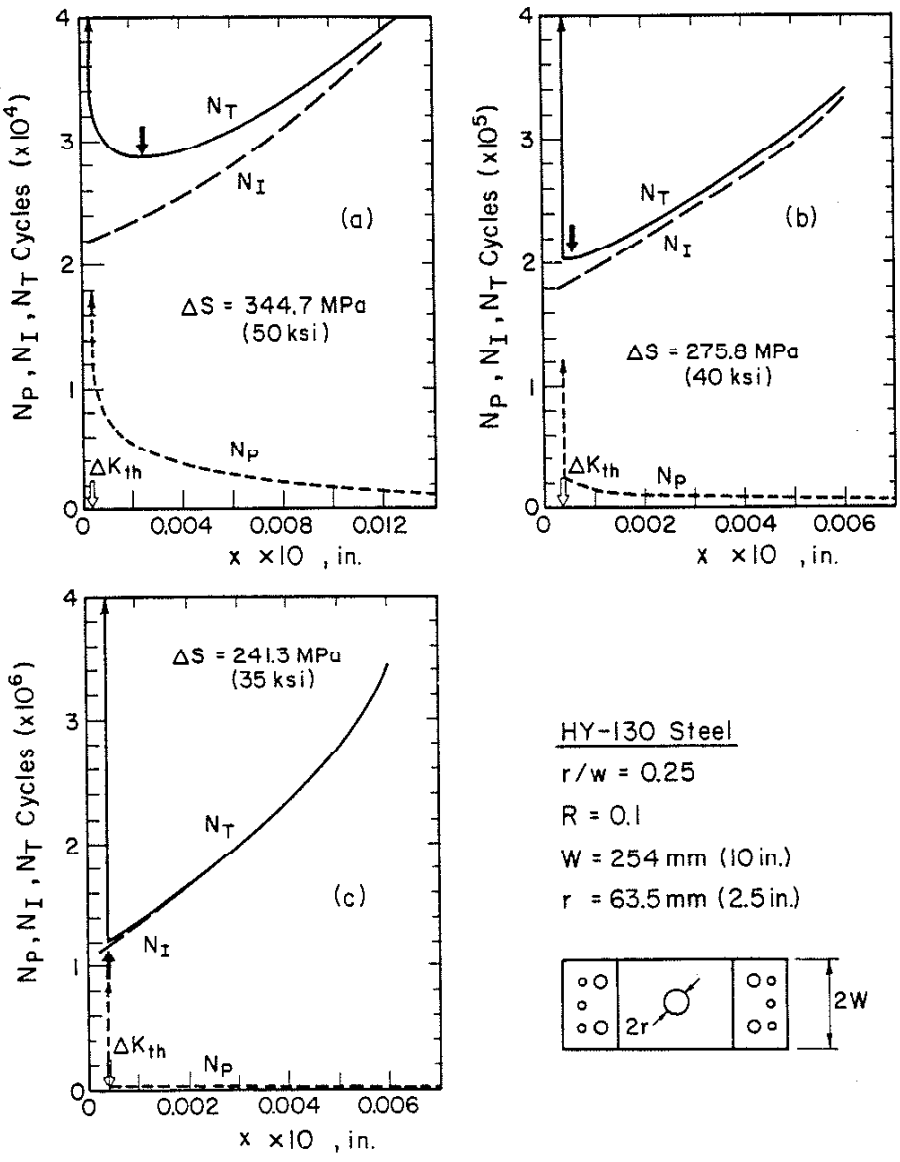

FIG. 4 APPLICATION OF CHEN'S a_I ESTIMATION METHOD TO A CIRCULARLY NOTCHED SPECIMEN AT VARIOUS STRESS LEVELS (23)

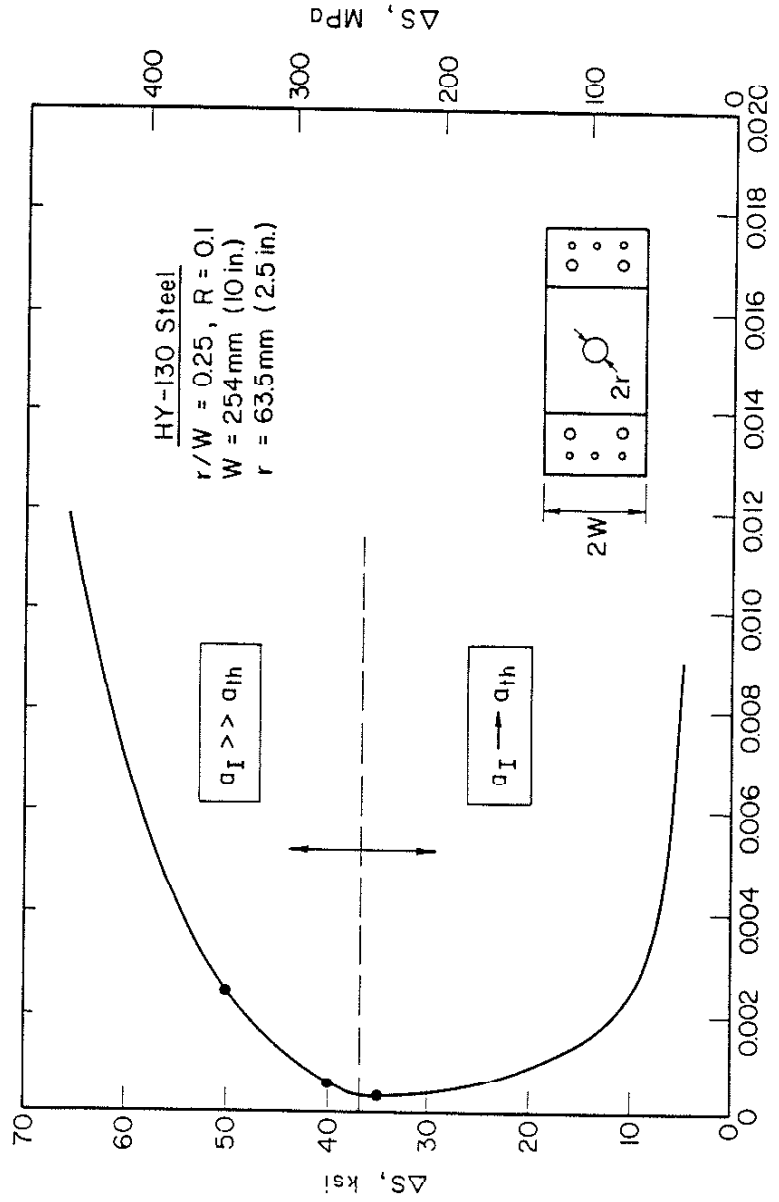

FIG. 5 PREDICTED CRACK INITIATION LENGTH (a_I) AS A FUNCTION OF APPLIED STRESS FROM FIG. 4 (23)

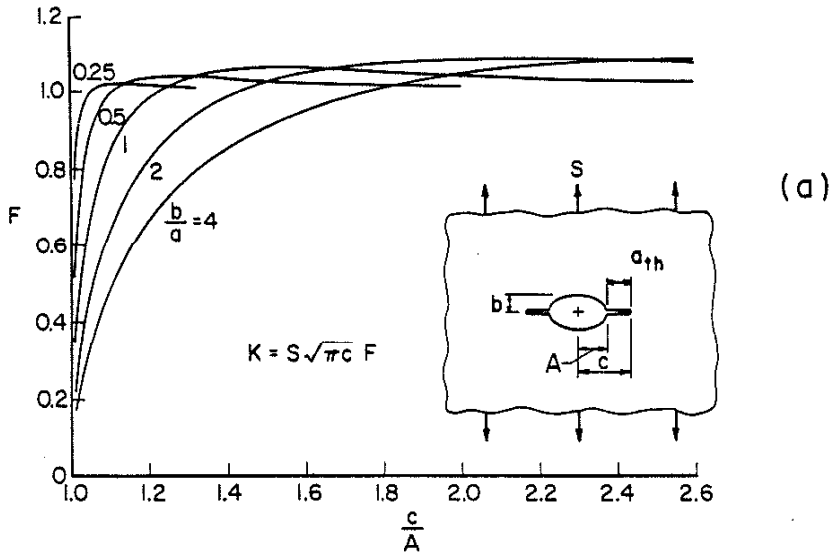

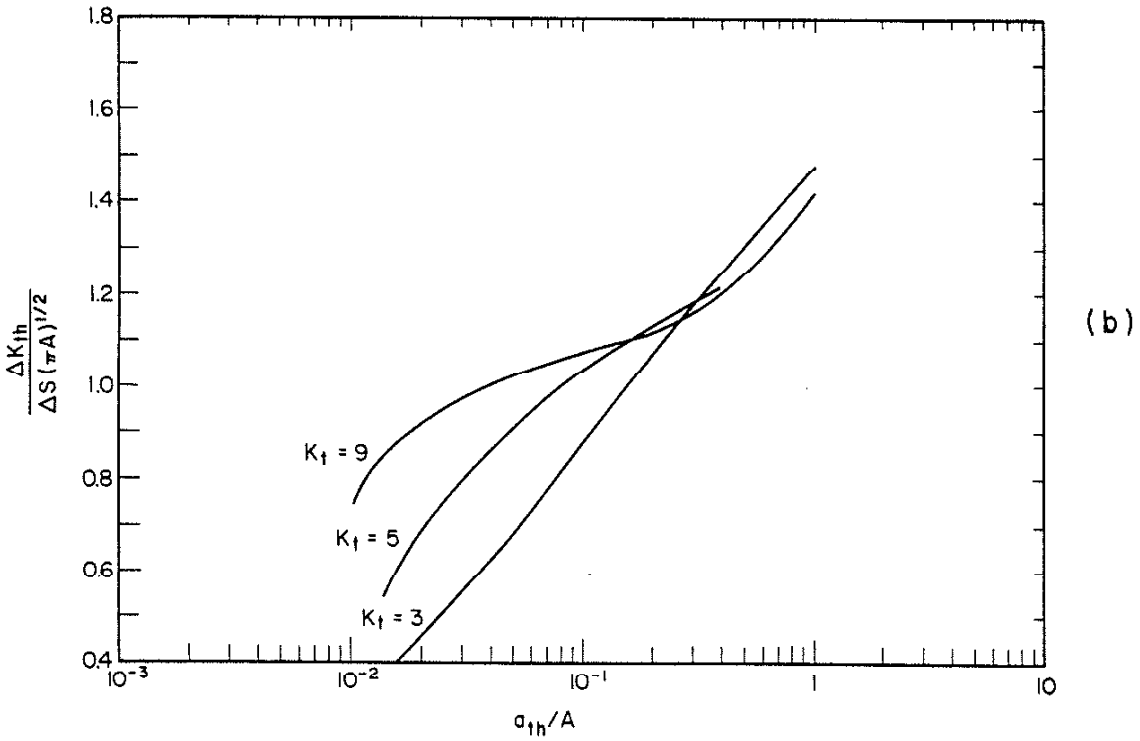

FIG. 6 STRESS INTENSITY CORRECTION FACTOR AND DIMENSIONLESS STRESS INTENSITY CORRECTION FACTOR FOR CRACKS EMANATING FROM AN ELLIPTICAL HOLE IN AN INFINITE PLATE (20)

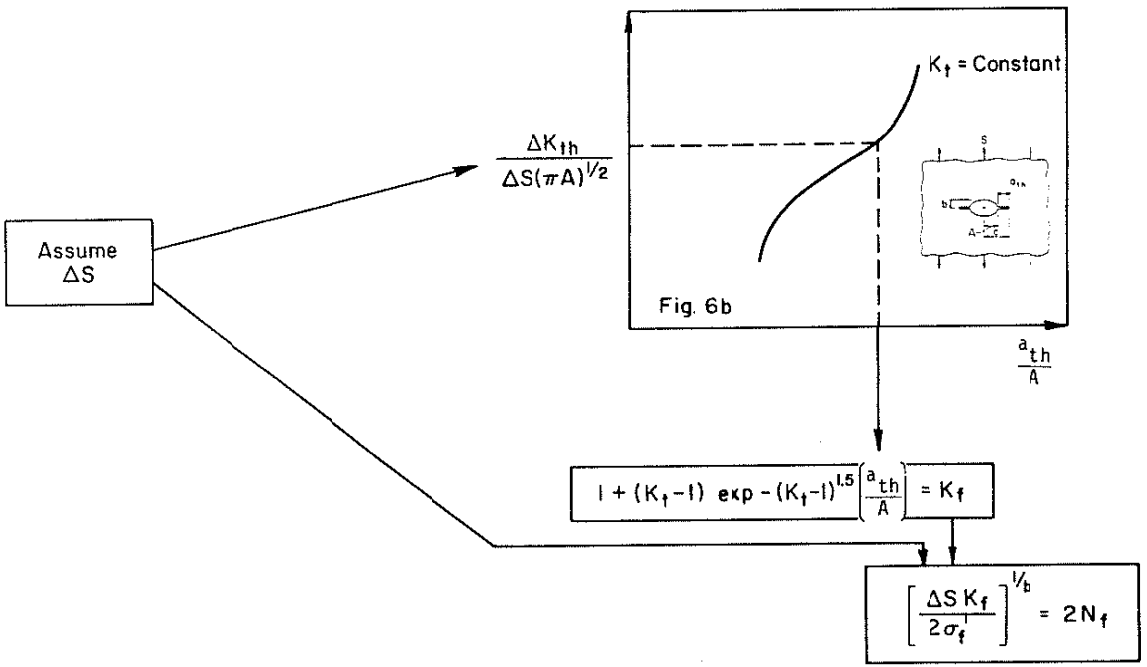

FIG. 7 SEQUENCE OF STEPS IN THE ESTIMATION OF K_f AND $2N_f$ CORRESPONDING TO AN ASSUMED VALUE OF ΔS

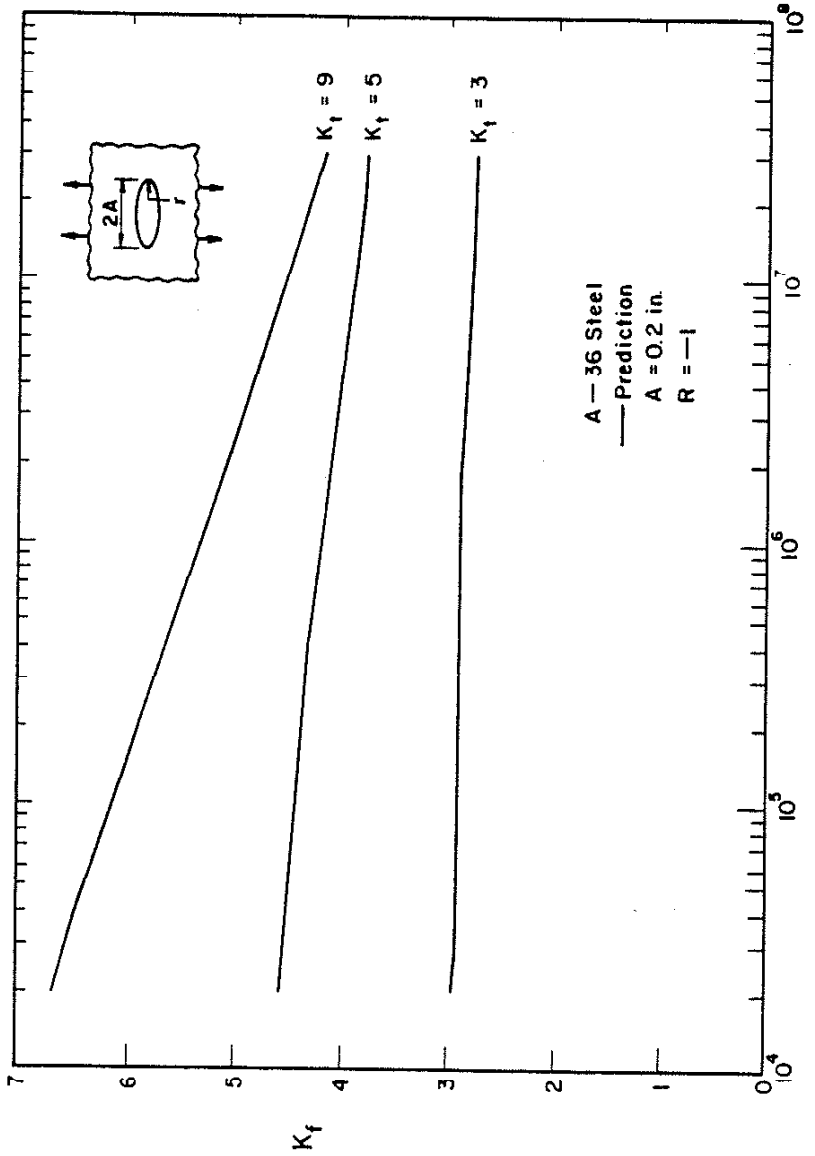

FIG. 8 PREDICTED VARIATION OF K_f WITH $2N_f$ AS A FUNCTION OF K_t FOR ELLIPTICALLY NOTCHED A-36 STEEL SPECIMENS

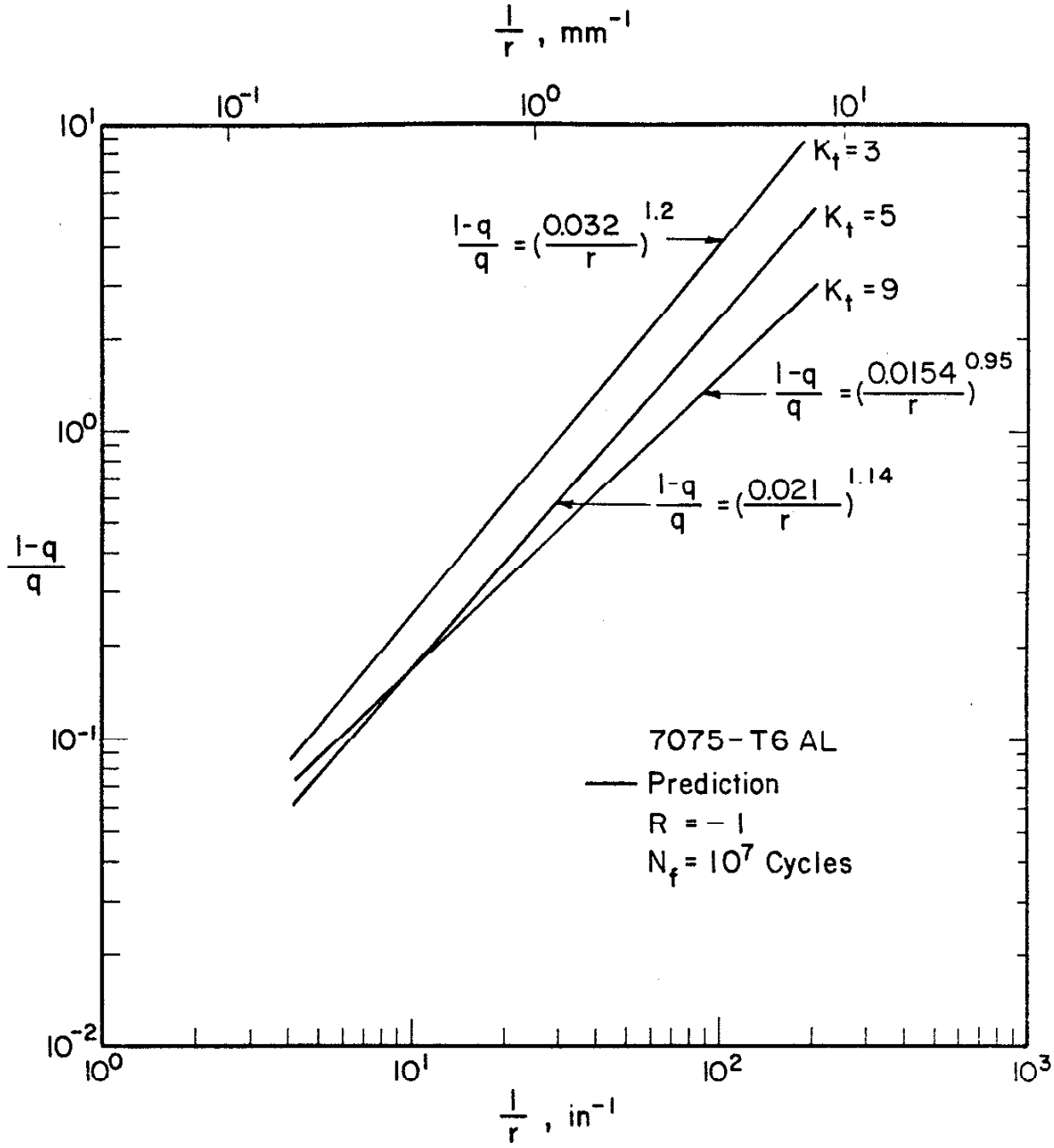

FIG. 9 INFLUENCE OF K_t ON THE PREDICTED VARIATION OF $(1 - q)/q$ AS A FUNCTION OF $1/r$ FOR GEOMETRICALLY SIMILAR NOTCHED 7075-T6 ALUMINUM ALLOY SPECIMENS

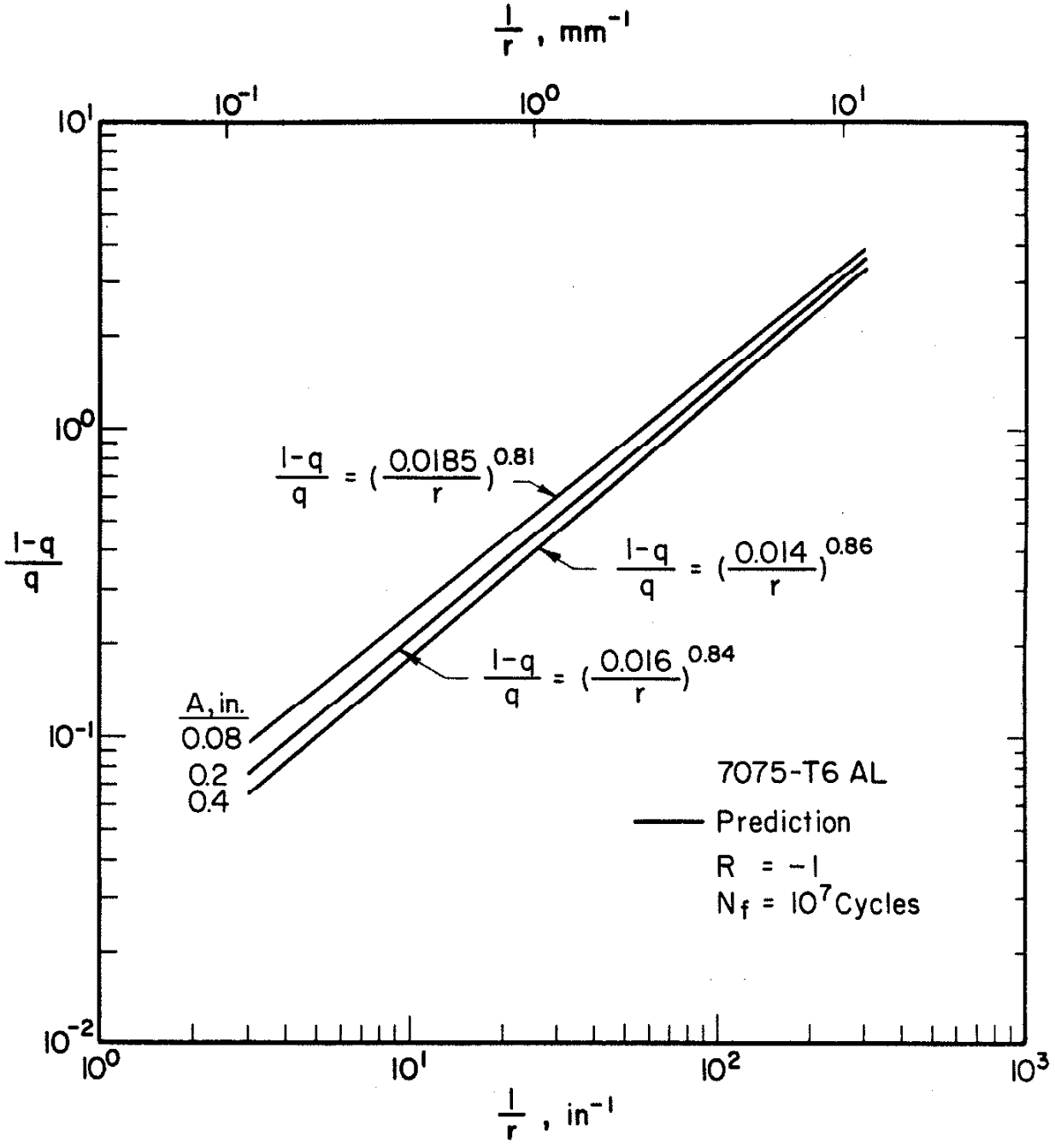

FIG. 10 INFLUENCE OF NOTCH DEPTH (A) ON THE PREDICTED VARIATION OF (1 - q)/q WITH 1/r FOR ELLIPTICALLY NOTCHED 7075-T6 ALUMINUM ALLOY SPECIMENS

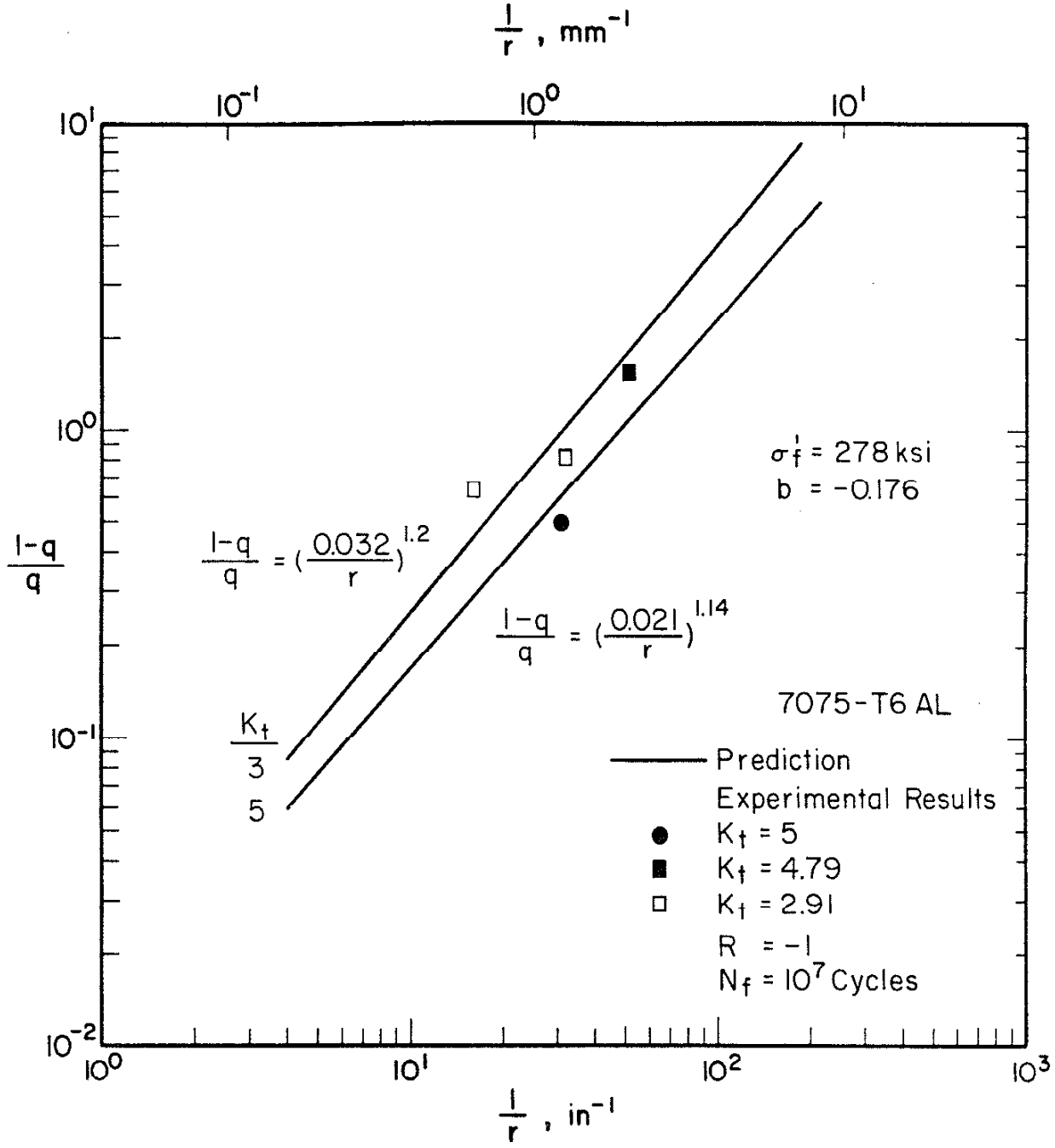

FIG. 11 COMPARISON OF PREDICTED VALUES OF (1 - q)/q AS A FUNCTION OF 1/r WITH EXPERIMENTAL VALUES FOR THE GEOMETRICALLY SIMILAR NOTCHED 7075-T6 ALUMINUM ALLOY SPECIMENS FROM REF. 4

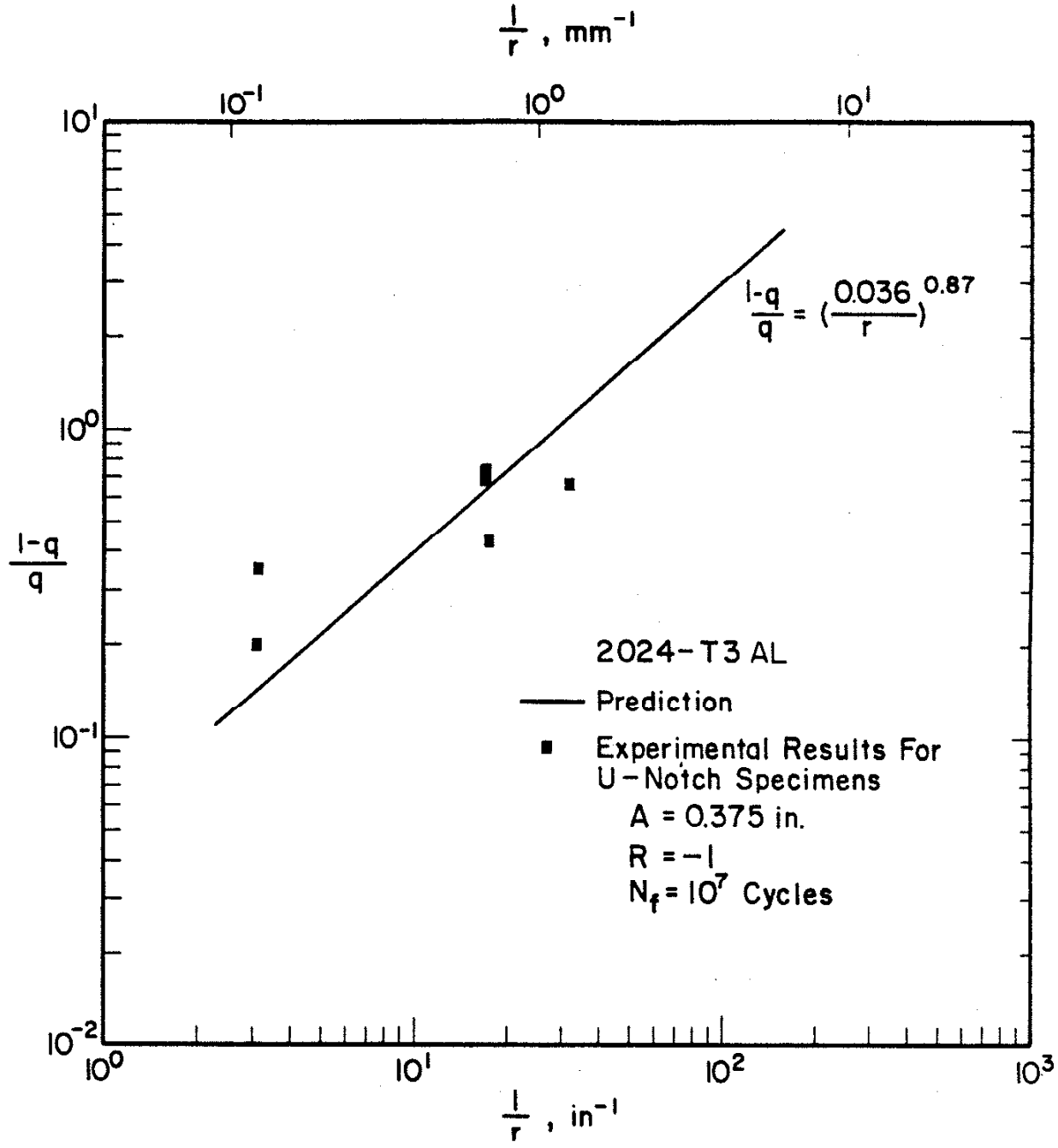

FIG. 12 COMPARISON OF PREDICTED VALUES OF (1 - q)/q AS A FUNCTION OF 1/r WITH EXPERIMENTAL VALUES FOR ELLIPTICALLY NOTCHED 2024-T3 ALUMINUM ALLOY SPECIMENS FROM REF. 4

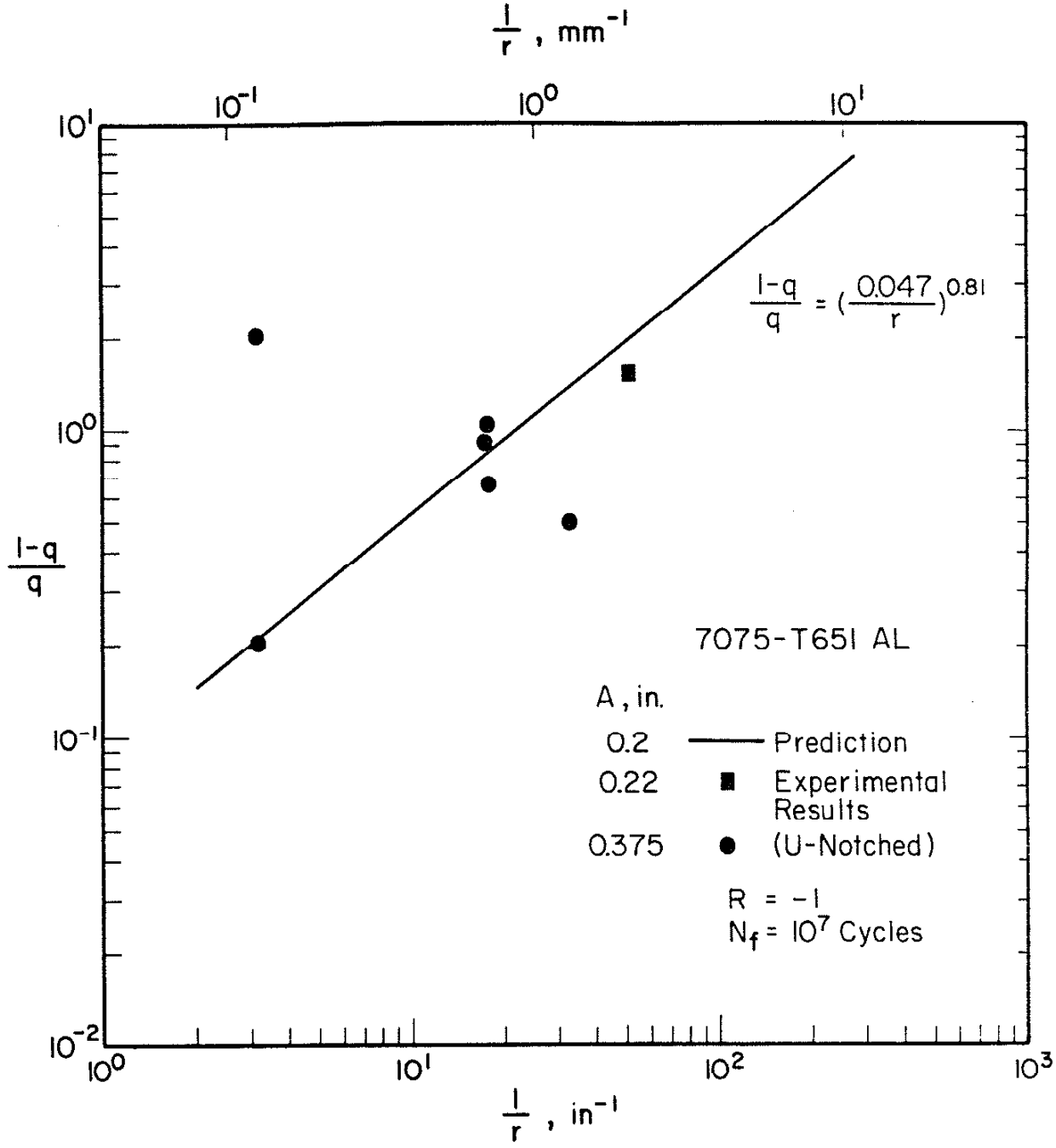

FIG. 13 COMPARISON OF PREDICTED VALUES OF (1 - q)/q AS A FUNCTION OF 1/r WITH EXPERIMENTAL VALUES FOR ELLIPTICALLY NOTCHED 7075-T651 ALUMINUM ALLOY SPECIMENS FROM REF. 4

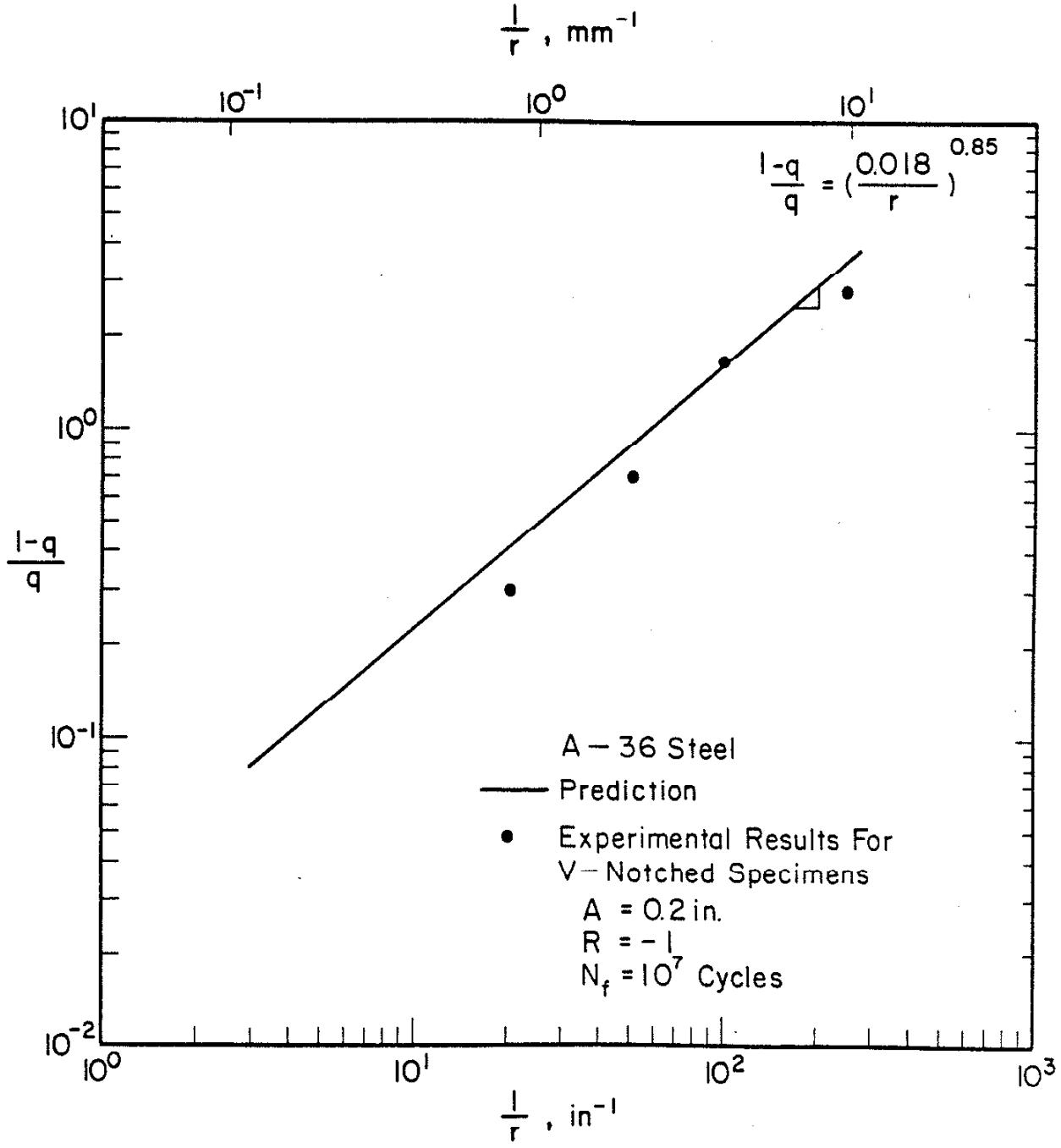

FIG. 14 COMPARISON OF PREDICTED VALUES OF (1 - q)/q AS A FUNCTION OF 1/r WITH EXPERIMENTAL VALUES FOR ELLIPTICALLY NOTCHED MILD STEEL SPECIMENS FROM REF. 24

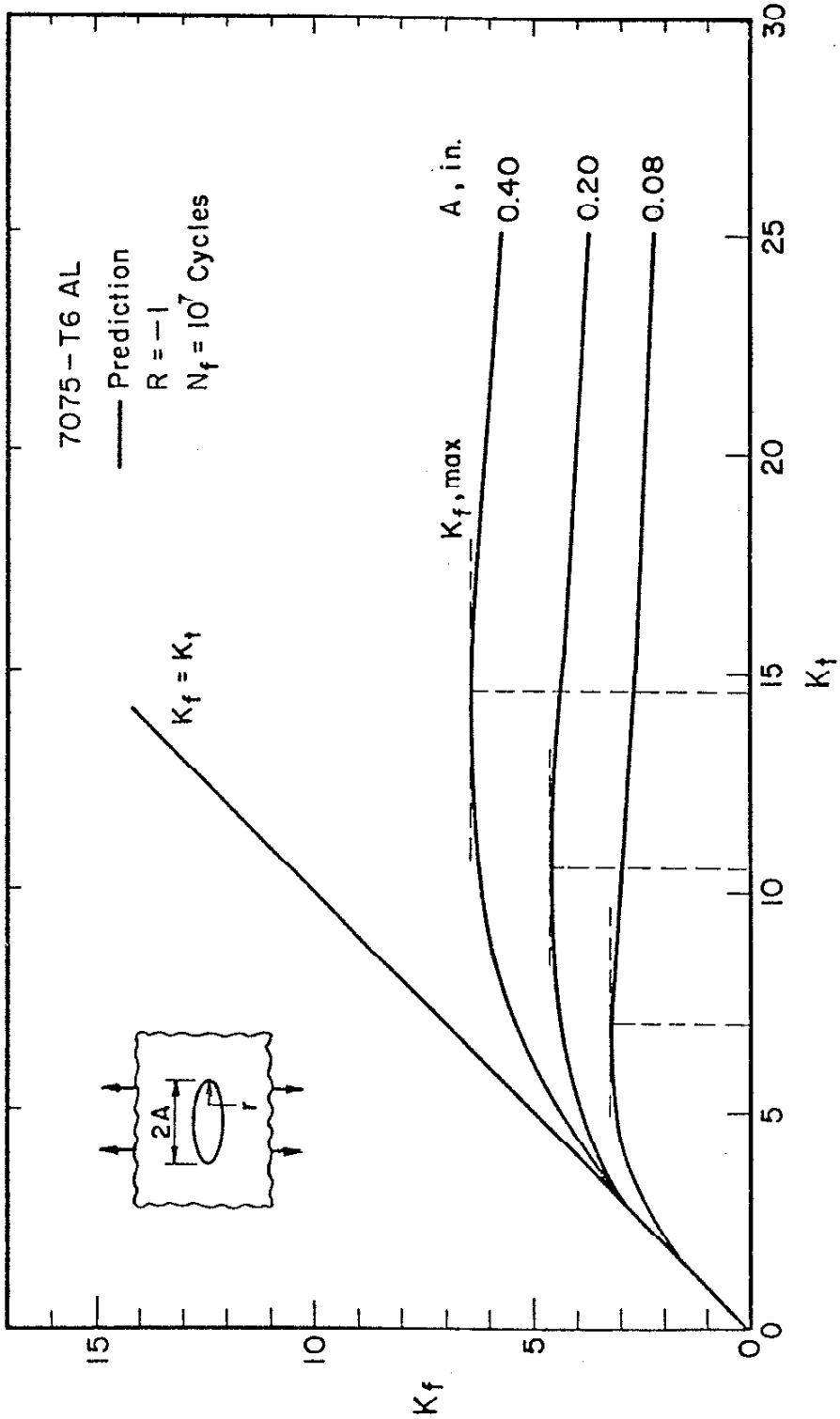

FIG. 15 PREDICTED VARIATION OF K_f WITH K_t FOR ELLIPTICALLY NOTCHED 7075-T6 ALUMINUM ALLOY SPECIMENS AS A FUNCTION OF NOTCH DEPTH (A)

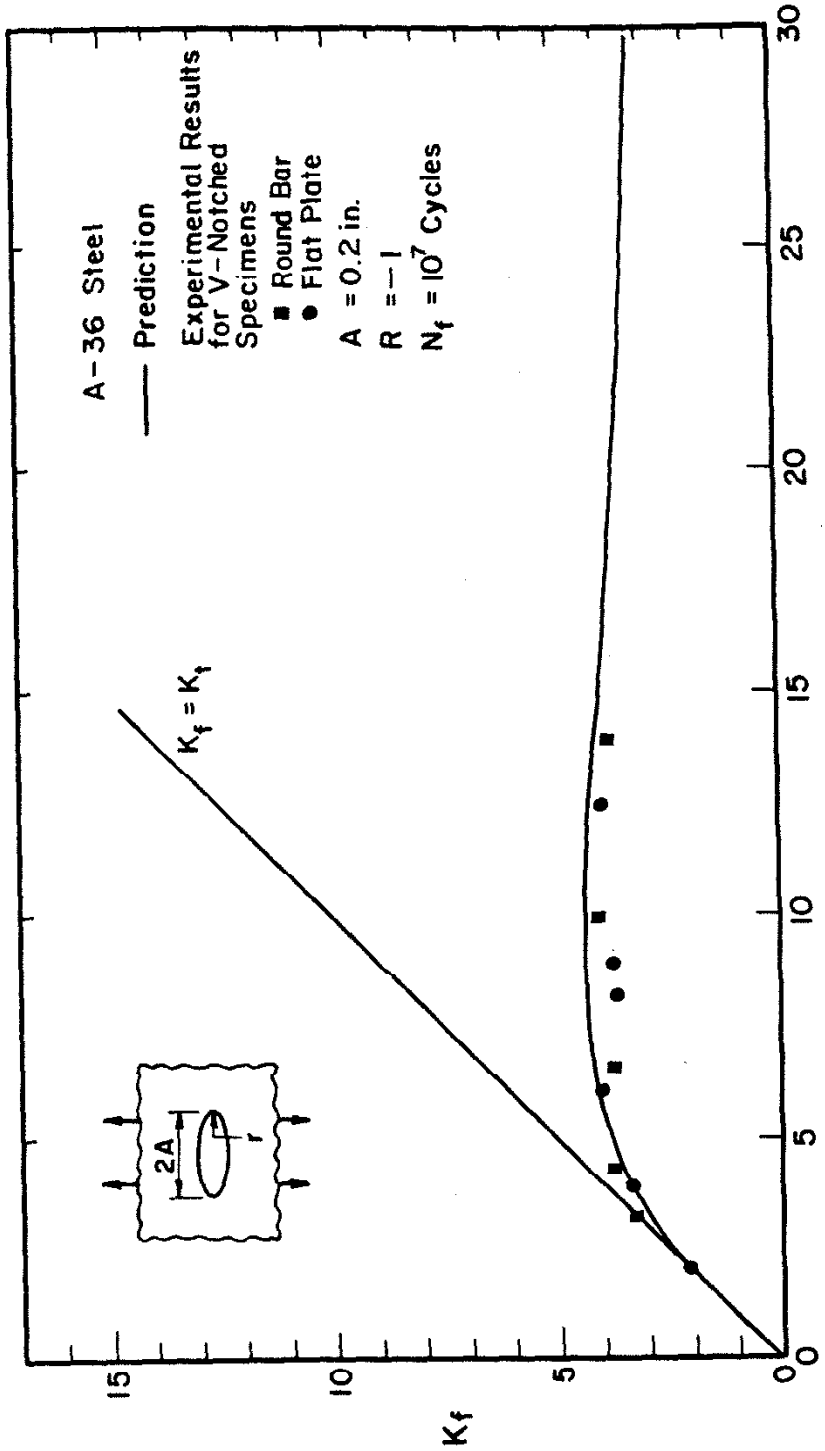

FIG. 16 COMPARISON OF PREDICTED VALUES OF K_f AS A FUNCTION OF K_t WITH EXPERIMENTAL VALUES FOR ELLIPTICALLY NOTCHED MILD STEEL SPECIMENS FROM REF. 24

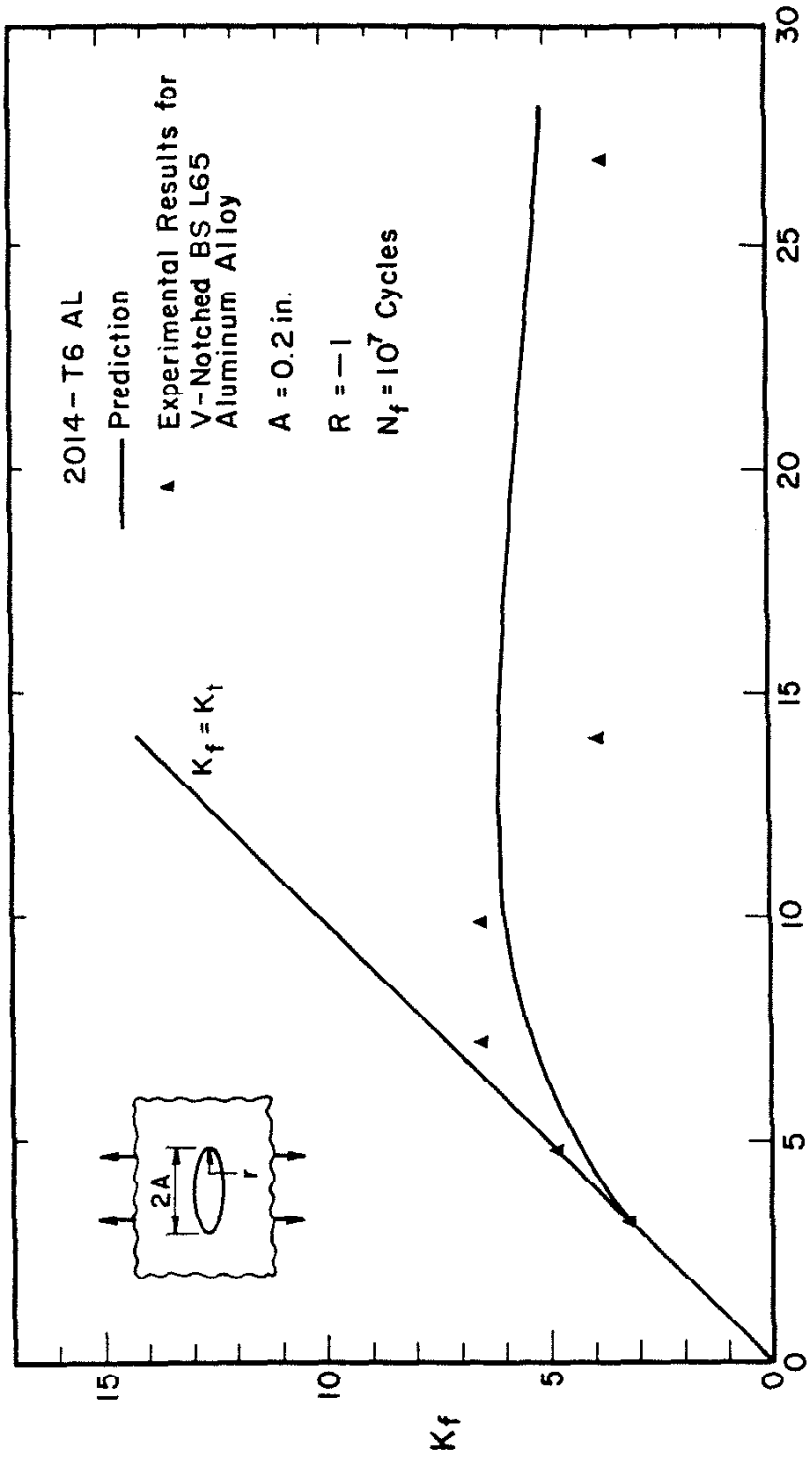

FIG. 17 COMPARISON OF PREDICTED VALUES OF K_f AS A FUNCTION OF K_t WITH EXPERIMENTAL VALUES FOR ELLIPTICALLY NOTCHED BS L65 ALUMINUM ALLOY SPECIMENS FROM REF. 25

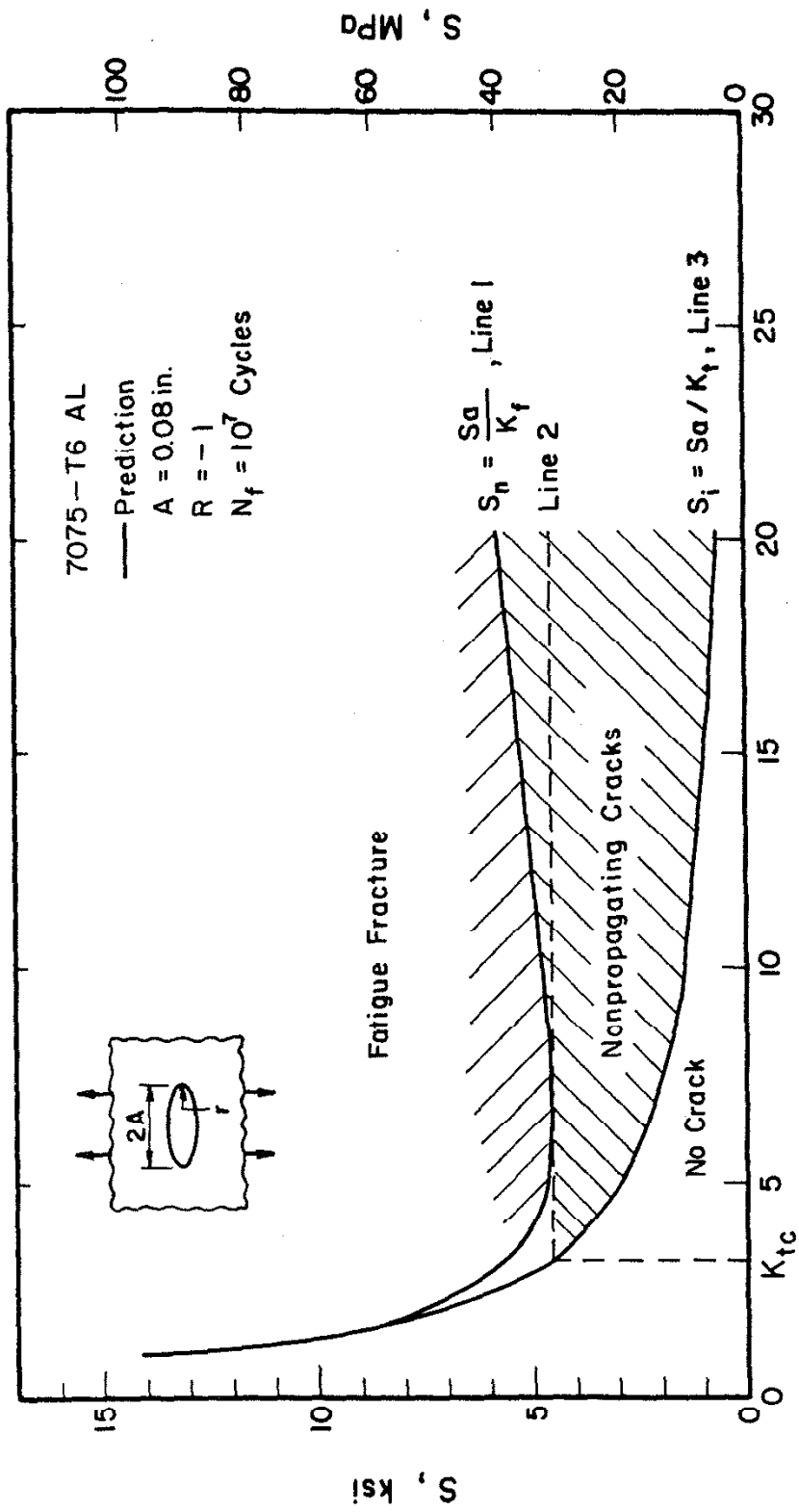

FIG. 18 PREDICTED VARIATION OF S_i AND S_n AS A FUNCTION OF K_t FOR ELLIPTICALLY NOTCHED 7075-T6 ALUMINUM ALLOY SPECIMENS

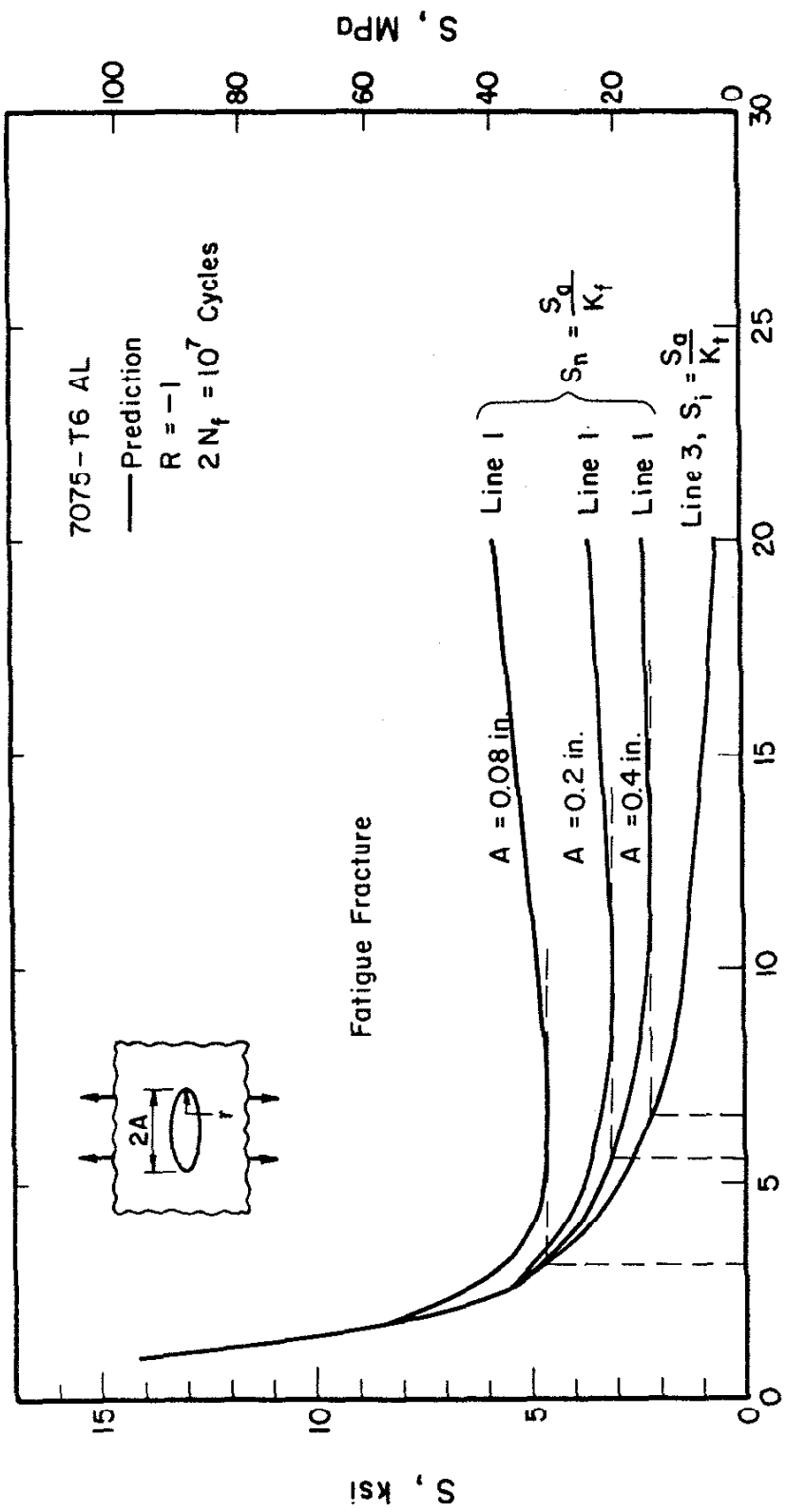

FIG. 19 PREDICTED INFLUENCE OF NOTCH DEPTH (A) ON S_n AS A FUNCTION OF K_t FOR ELLIPTICALLY NOTCHED 7075-T6 ALUMINUM ALLOY SPECIMENS

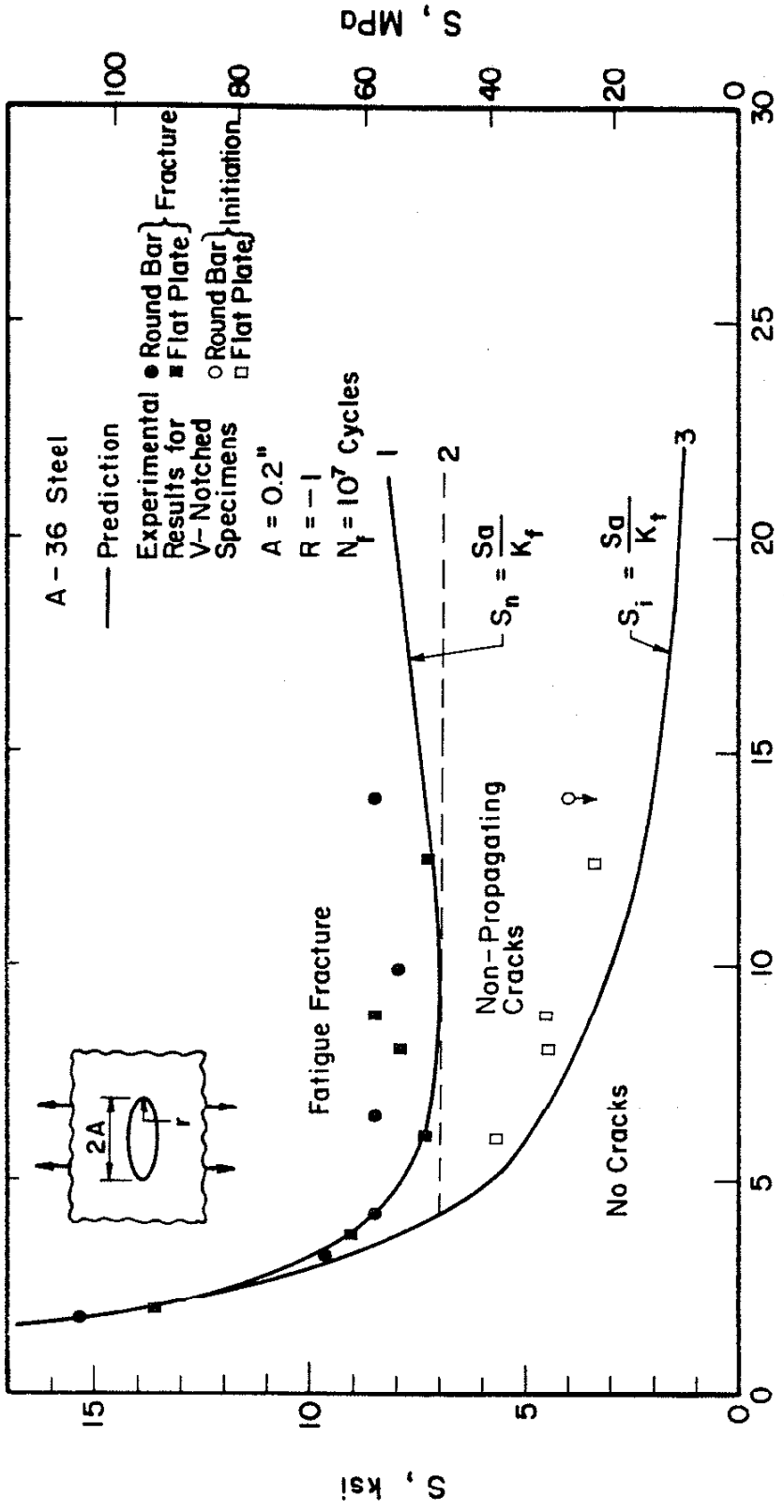

FIG. 20 COMPARISON OF PREDICTED VALUES OF S_i AND S_n AS A FUNCTION OF K_t WITH EXPERIMENTAL RESULTS FOR ELLIPTICALLY NOTCHED MILD STEEL SPECIMENS FROM REF. 24

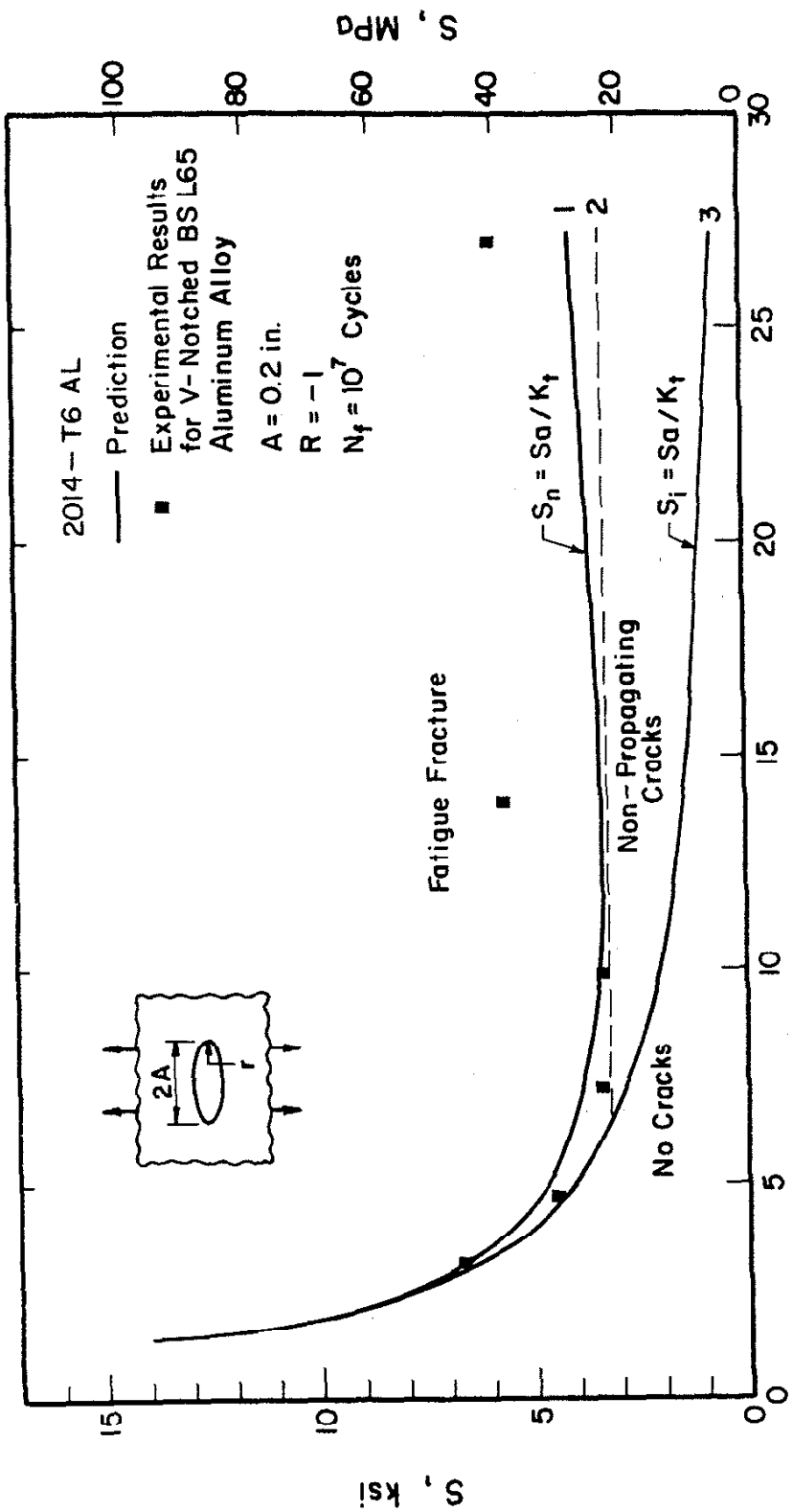

FIG. 21 COMPARISON OF PREDICTED VALUES OF S_i AND S_n AS A FUNCTION OF K_t WITH EXPERIMENTAL RESULTS FOR ELLIPTICALLY NOTCHED BS L65 ALUMINUM ALLOY SPECIMENS FROM REF. 25

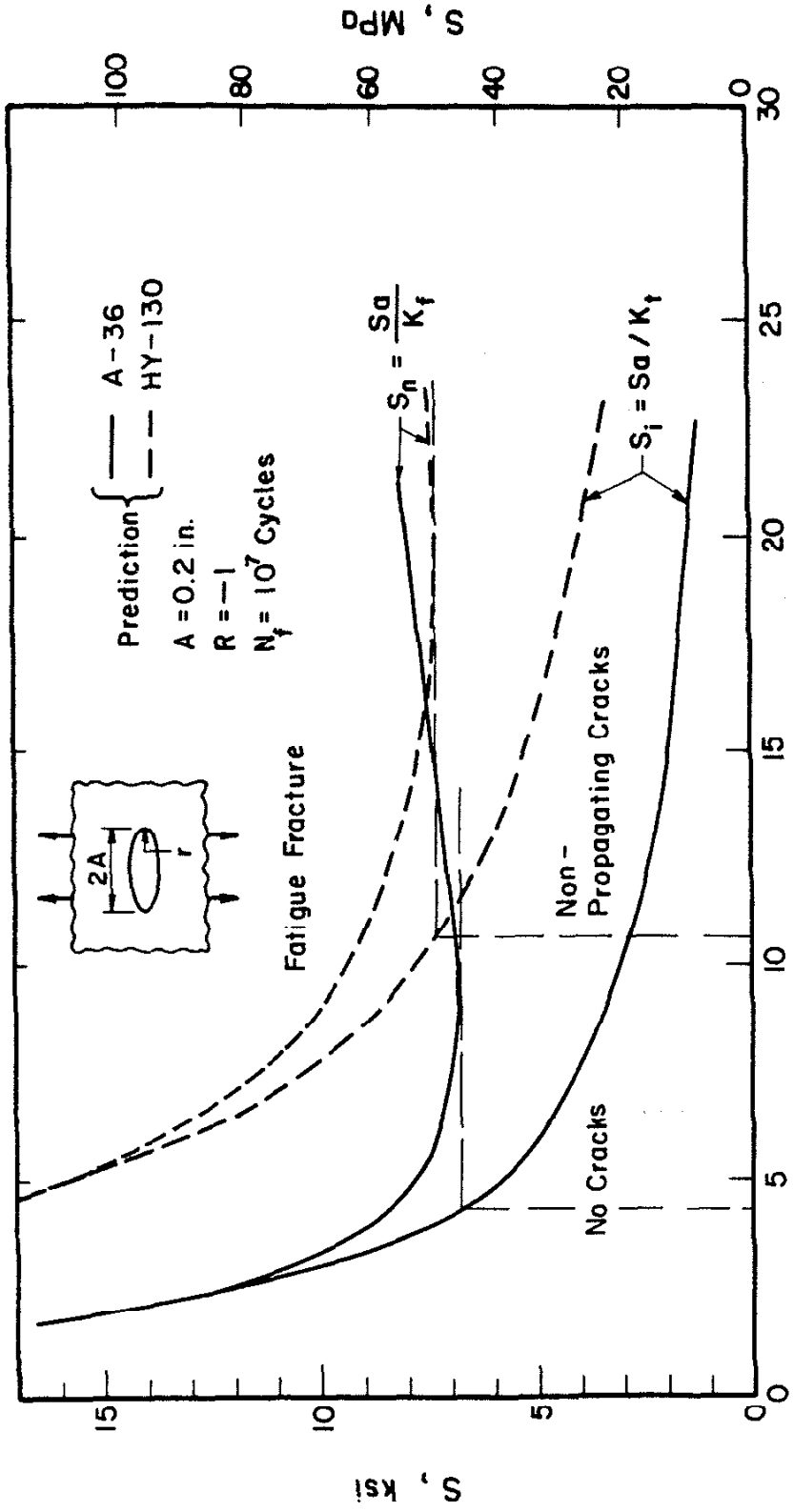

FIG. 22 ILLUSTRATION OF THE INFLUENCE OF THE MATERIAL PROPERTIES ON THE FORMATION OF THE NONPROPAGATING CRACKS

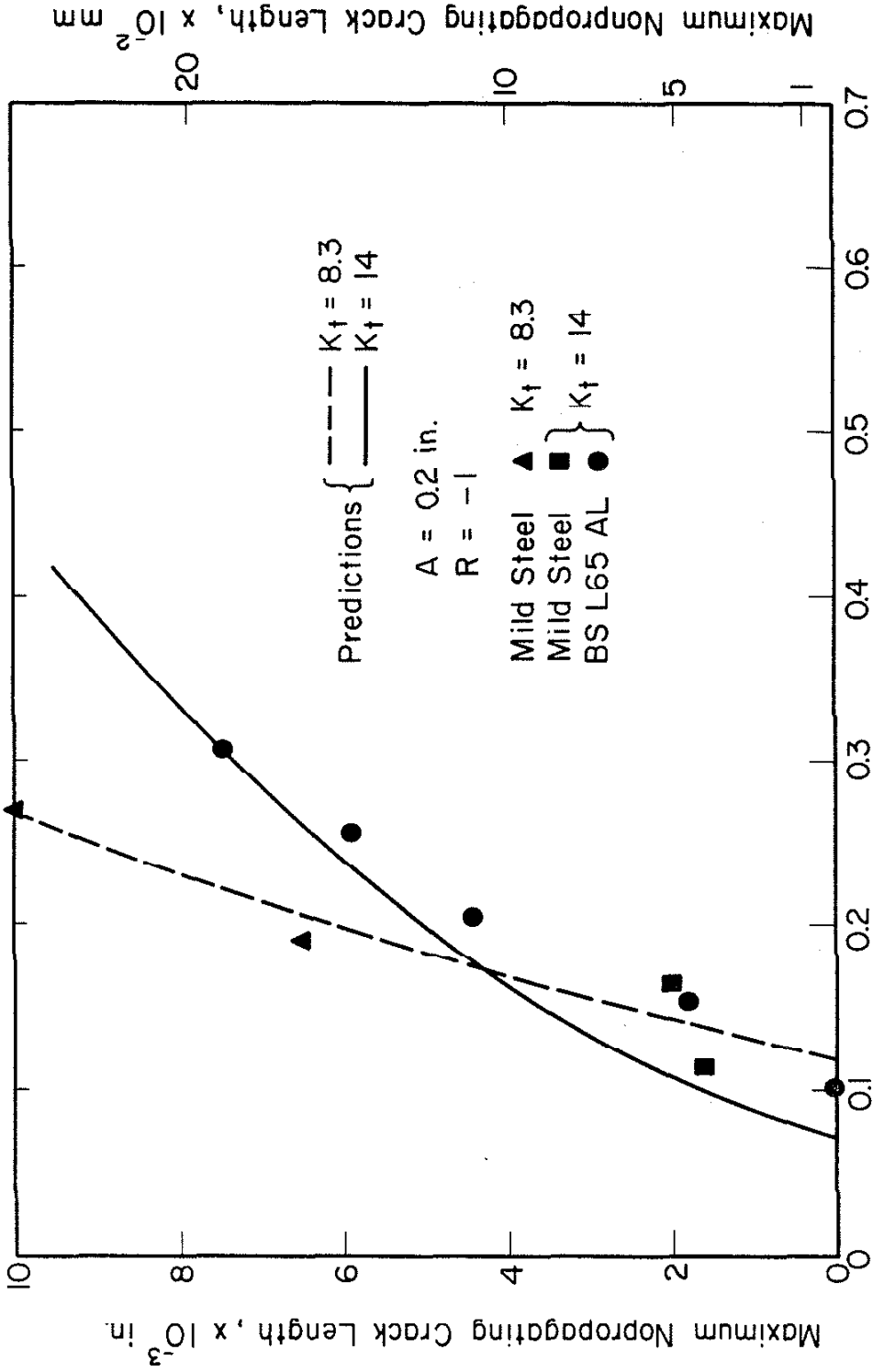

FIG. 23 COMPARISON OF VALUES OF THE MAXIMUM LENGTH OF THE NONPROPAGATING CRACKS AS A FUNCTION OF STRESS LEVEL WITH THE EXPERIMENTAL RESULTS FROM REFS. 17 AND 27

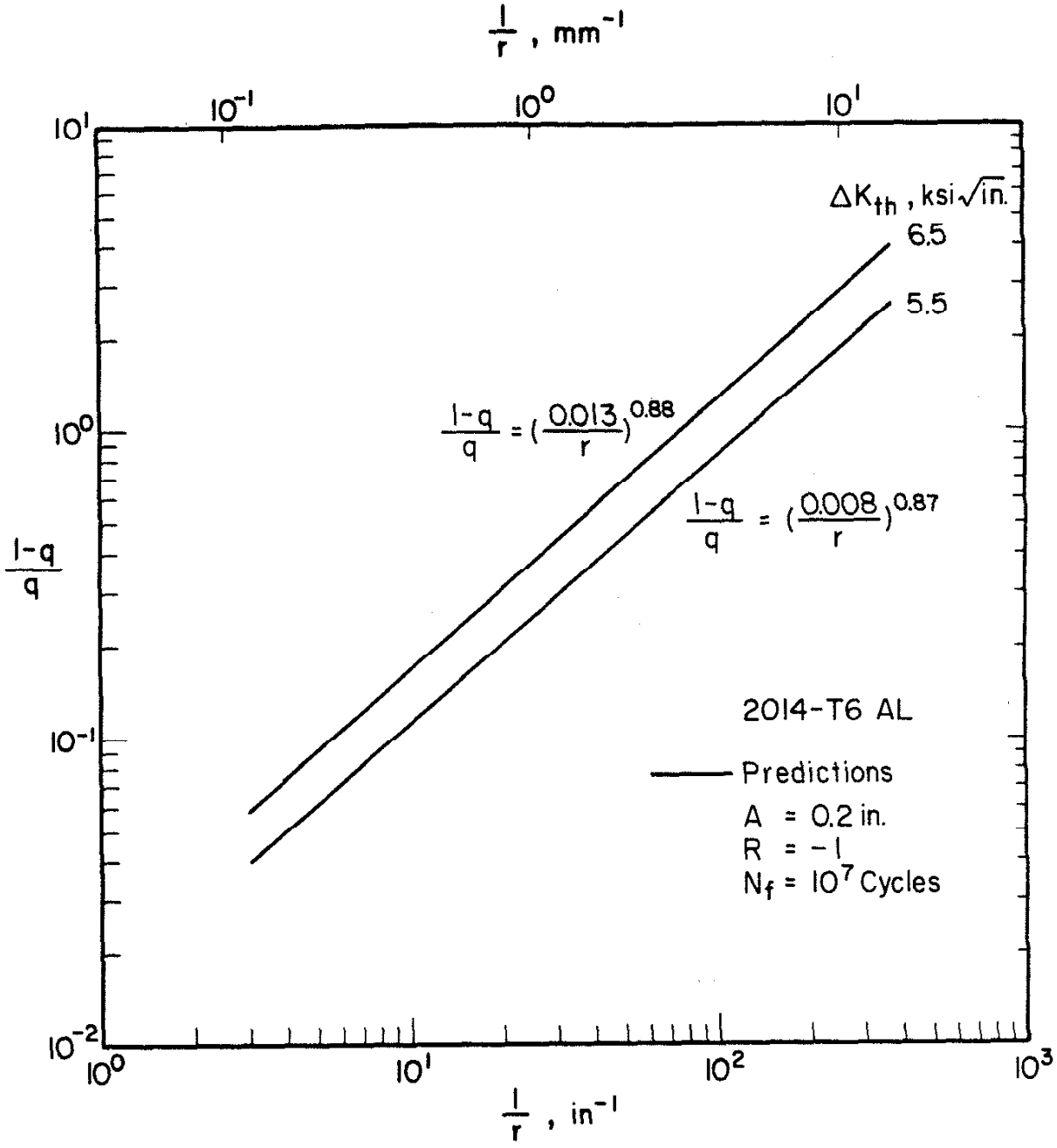

FIG. 24 EFFECT OF ΔK_{th} ON THE PREDICTED VARIATION OF $(1 - q)/q$ AS A FUNCTION OF $1/r$ FOR ELLIPTICALLY NOTCHED 2014-T6 ALUMINUM ALLOY SPECIMENS

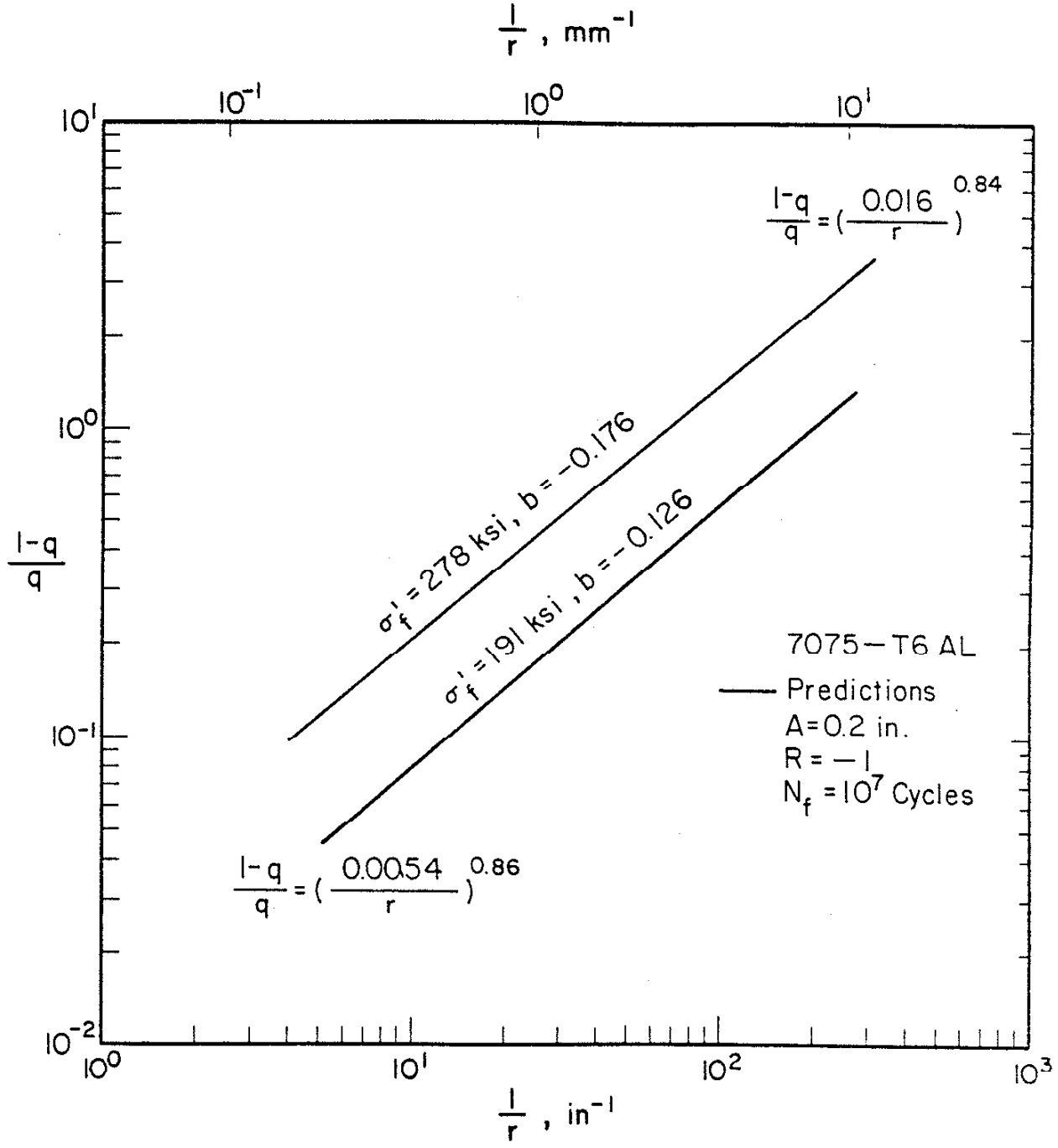

FIG. 25 PREDICTED EFFECT OF MATERIAL PROPERTIES ON THE VARIATION OF $(1 - q)/q$ AS A FUNCTION OF $1/r$ FOR ELLIPTICALLY NOTCHED ALUMINUM ALLOY SPECIMENS

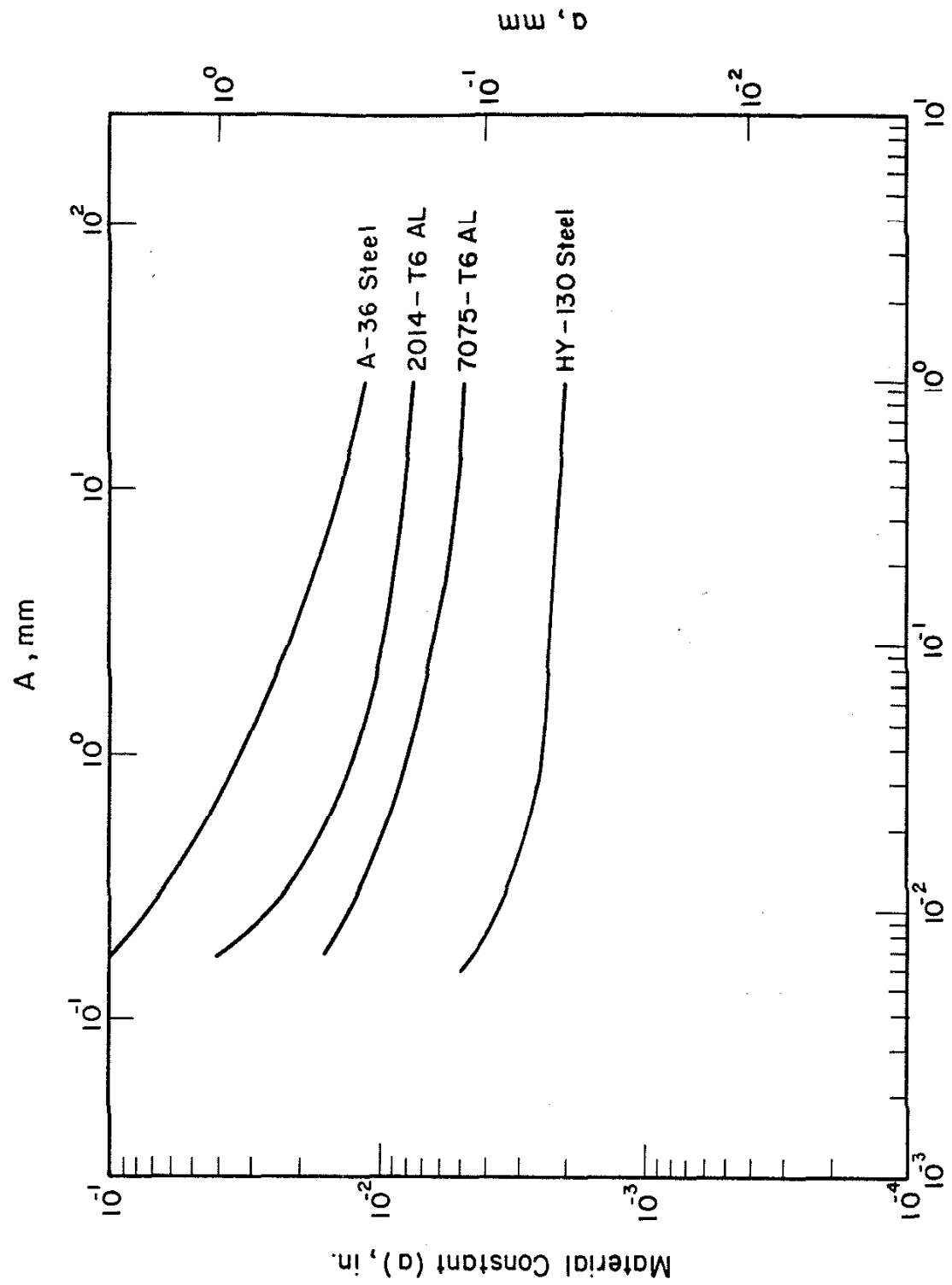

FIG. 26 PREDICTED INFLUENCE OF NOTCH DEPTH (A) ON THE MATERIAL CONSTANT (a) FOR ELLIPTICALLY NOTCHED STEELS AND ALUMINUM ALLOYS

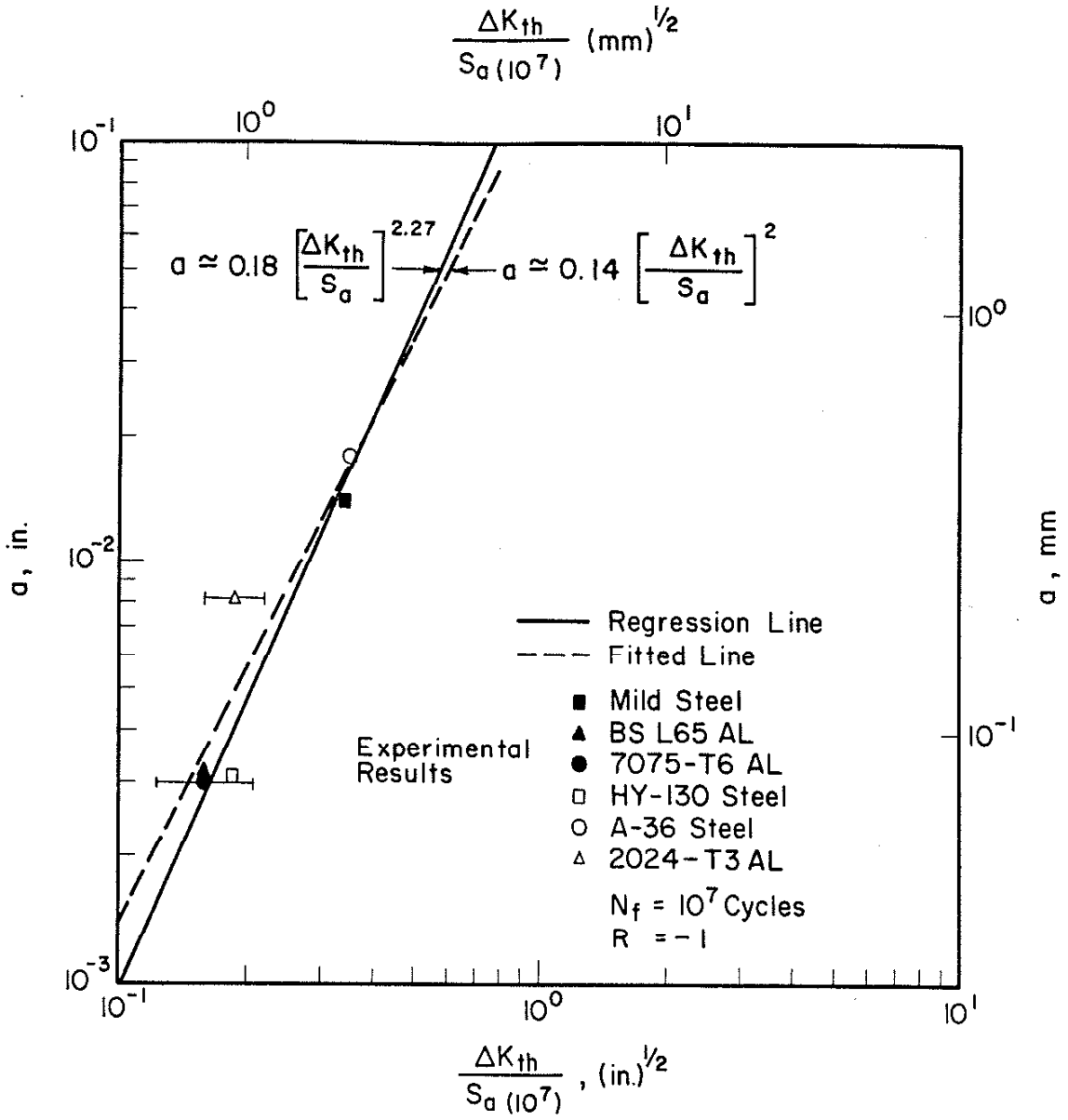

FIG. 27 COMPARISON OF PREDICTED VALUES OF MATERIAL CONSTANT (a) AS A FUNCTION OF $\Delta K_{th}/S_a$ WITH EXPERIMENTALLY REPORTED VALUES OF a, ΔK_{th} and S_a FROM REFS. 4, 6, 18, 23, 24, 25, 30, 31, 40, 41 42, 43 and 49.

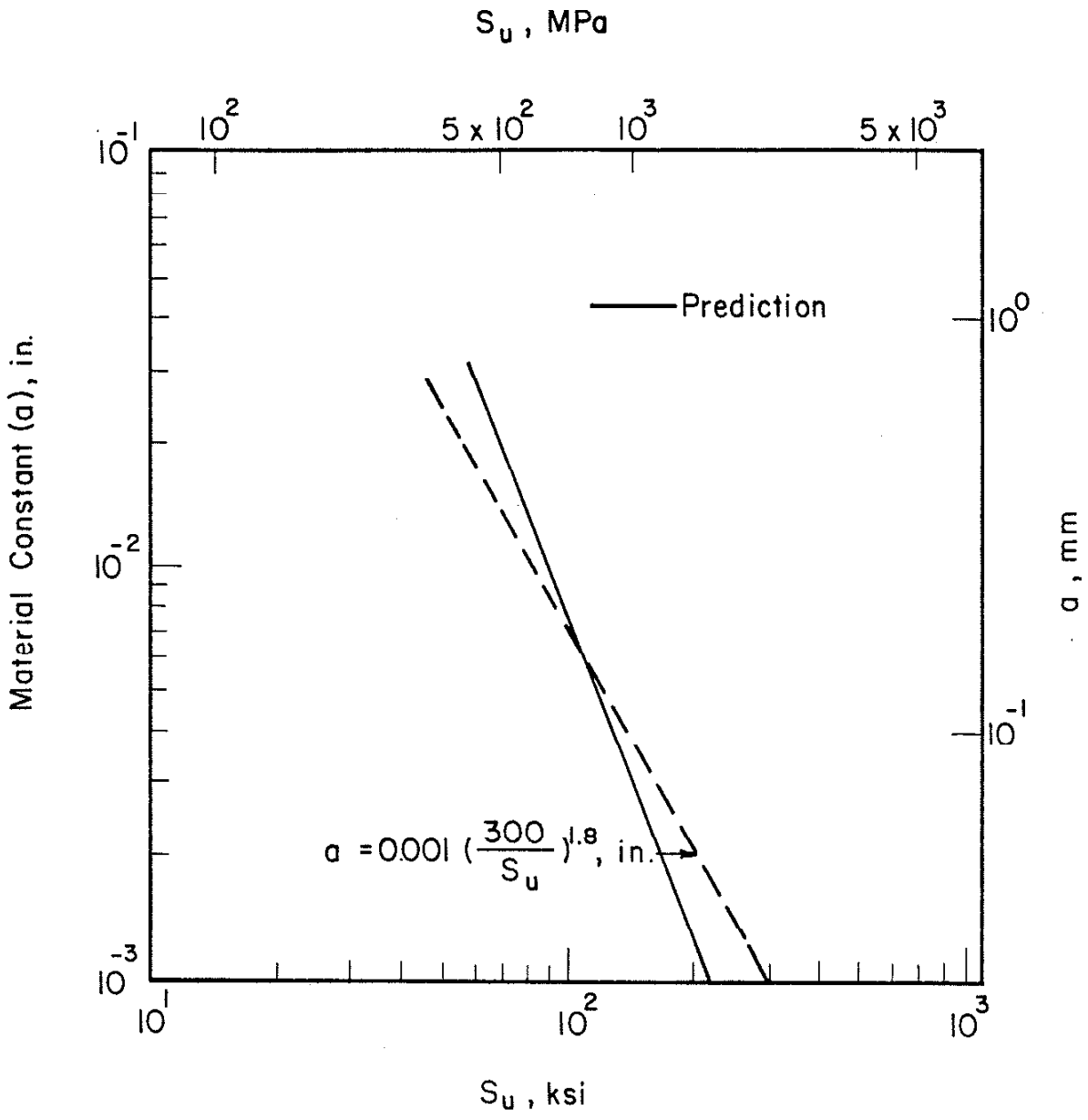

FIG. 28 COMPARISON OF THE VALUES OF MATERIAL CONSTANT (a) PREDICTED USING THE PRESENT ANALYTICAL MODEL AS A FUNCTION OF S_u WITH THE VALUES ESTIMATED USING EQ. 4.

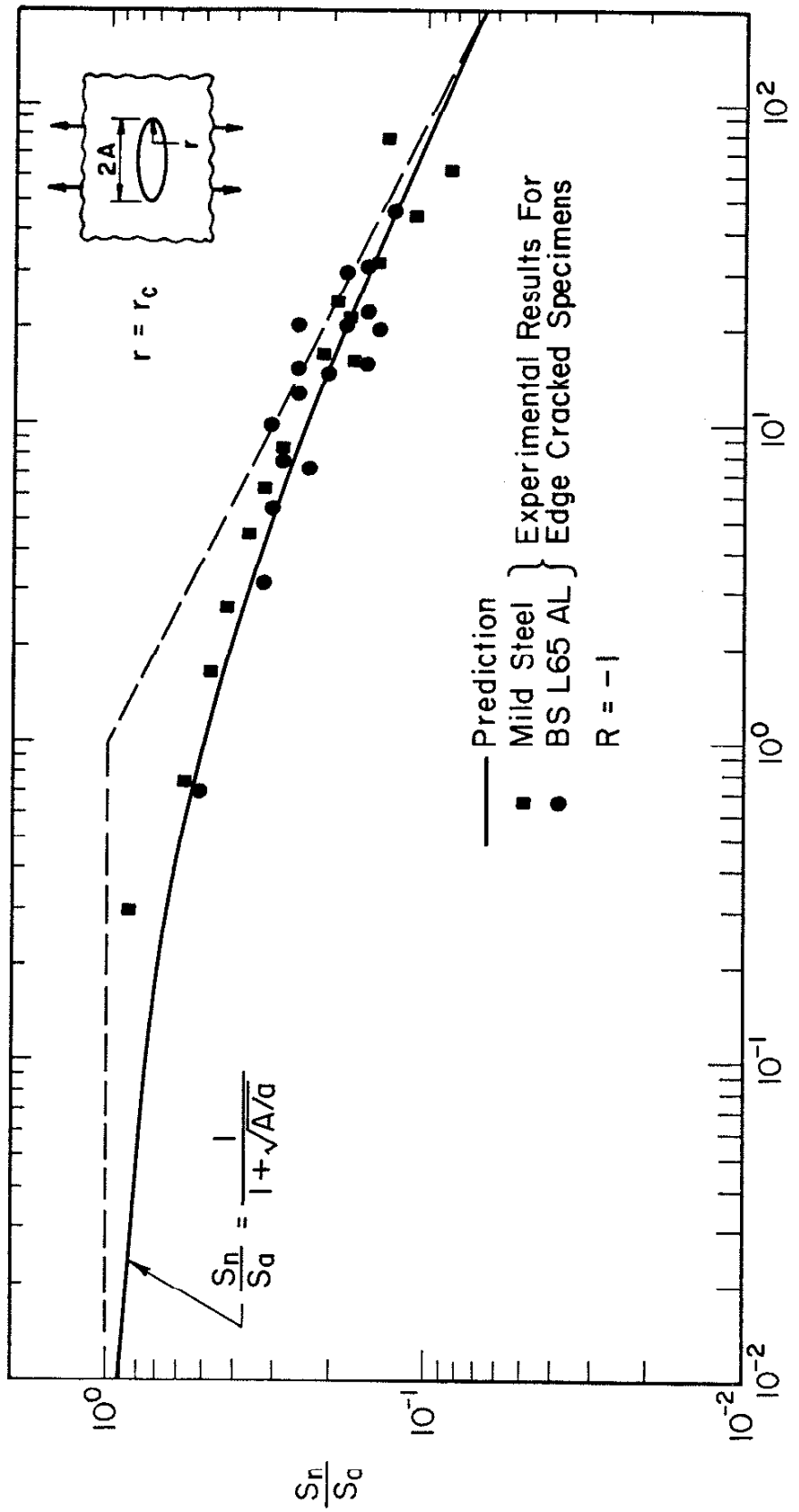

FIG. 29 COMPARISON OF S_n/S_a AS A FUNCTION OF A/a PREDICTED USING EQ. 33 FOR NOTCHED SPECIMENS WITH THE EXPERIMENTAL RESULTS OF EDGE-CRACKED, MILD-STEEL AND BS L65 ALUMINUM ALLOY SPECIMENS FROM REFS. 24 AND 34

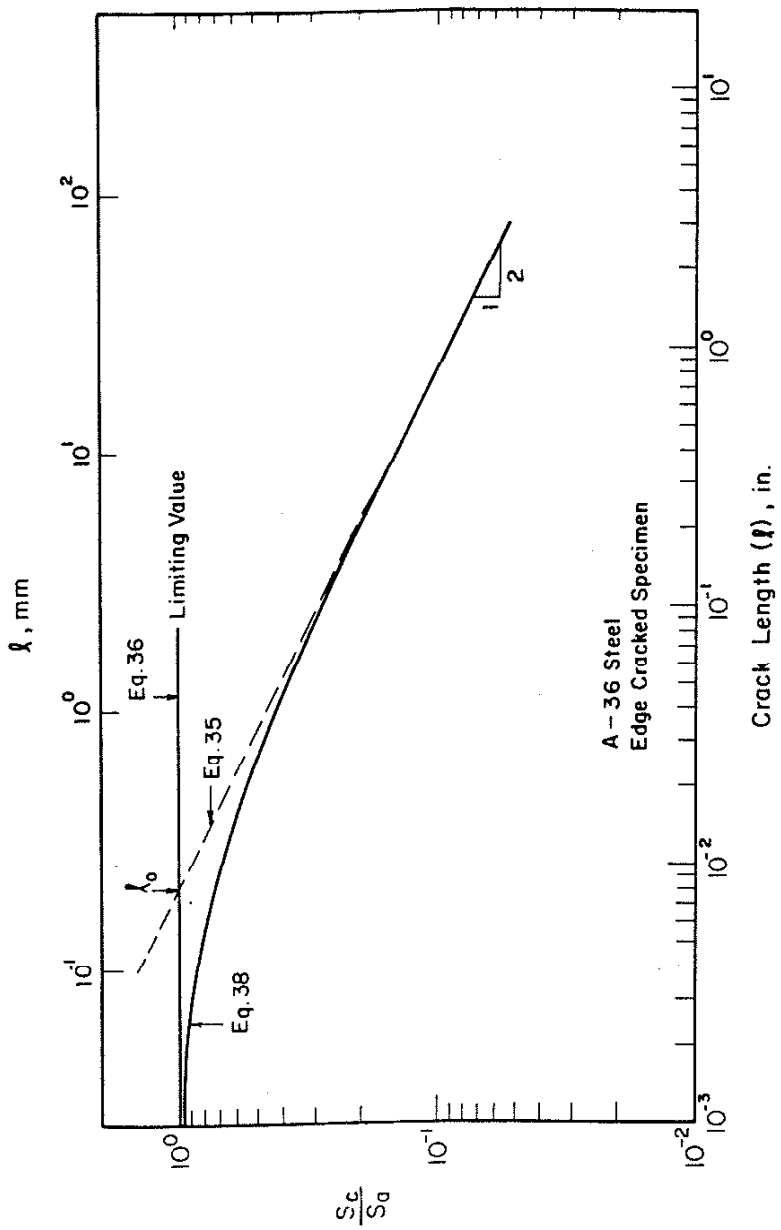

FIG. 30 EVALUATION OF THE INTRINSIC CRACK LENGTH (ℓ_o) (30, 31)

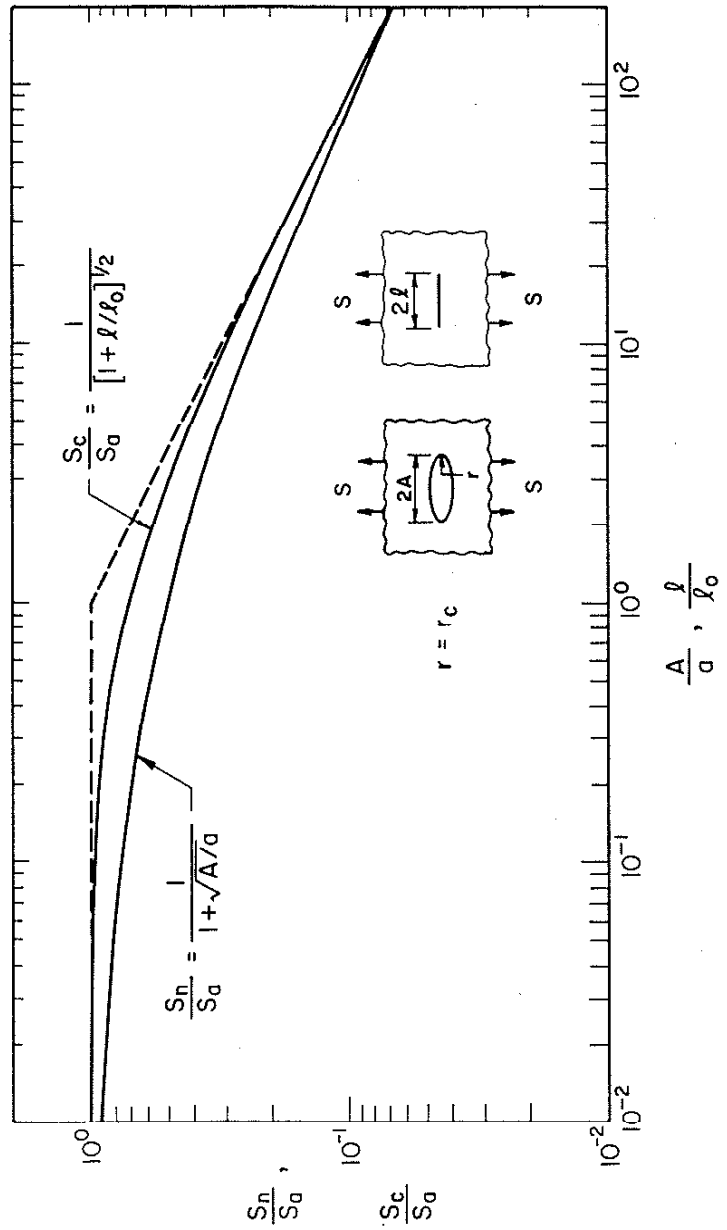

FIG. 31 ILLUSTRATION OF THE VARIATION OF S_n/S_a WITH A/a and S_c/S_a WITH ℓ/ℓ_0

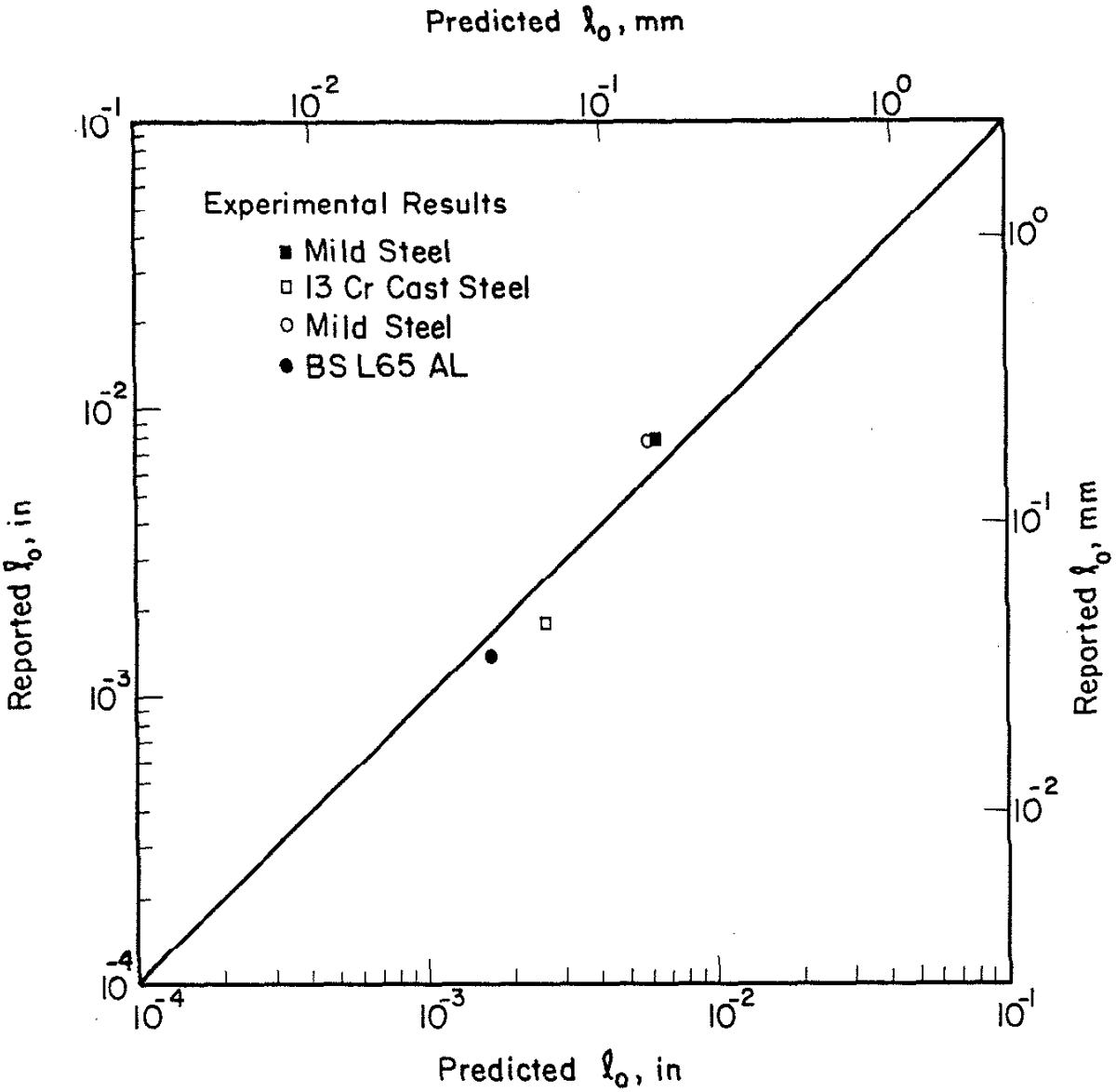

FIG. 32 COMPARISON OF PREDICTED VALUES OF THE INTRINSIC CRACK LENGTH (ℓ_o) FROM S_u AND EQS. 4 AND 42 WITH EXPERIMENTAL VALUES OF ℓ_o FROM REFS. 30, 31 AND 44

APPENDIX

STRESS-STRAIN DISTRIBUTION AHEAD OF A NOTCH

Figures A-1 and A-2 show the stress and strain distribution as a function of distance from the notch root for an aluminum alloy with an elliptical notch based on an elasto-plastic finite element analysis (45). While Fig. A-3 shows the normalized stress-strain distribution ahead of a notch root for different nominal stress ranges (ΔS) and has the following features:

(i) at the notch root, the normalized stress-strain distribution becomes one;

(ii) at very long distances from the notch root, theoretically such distribution should reach a limiting value of $1/K_t$;

(iii) the decay of the normalized stress-strain distribution has been assumed to an exponential and characterized by a gradient β at $x/A = 0$.

Then such distribution can be formulated as:

$$\frac{{}^{*}N\left(\frac{x}{A}\right)}{N(0)} - \frac{N\left(\frac{\infty}{A}\right)}{N(0)} = \left[1 - \frac{N\left(\frac{\infty}{A}\right)}{N(0)}\right] \exp - \beta\left(\frac{x}{A}\right) \qquad \text{(A-1)}$$

where $\{N(x/A)/N(0)\}$ is the normalized stress-strain parameter at a normalized distance x/A from the notch root.

Multiplying both sides by $\{N(0)/N(\infty/A)\}$, then Eq. A-1 can be written as:

---

*$N(x/A = [\Delta\sigma(x/A)\ \Delta\varepsilon(x/A)\ E]^{\frac{1}{2}}$; $N(0) = [\Delta\sigma(0)\ \Delta\varepsilon(0)\ E]^{\frac{1}{2}}$; and $N(\infty/A) = [\Delta\sigma(\infty/A)\ \Delta\varepsilon(\infty/A)\ E]^{\frac{1}{2}}$.

$$\left[\frac{N\left(\frac{x}{A}\right)}{N\left(\frac{\infty}{A}\right)}\right] - 1 = (K_t - 1) \exp - \beta\left(\frac{x}{A}\right) \qquad (A\text{-}2)$$

so, the slope of the plot between $\ell n[\{N(x/A)/N(\infty/A)\} - 1]$ and x/A will give β (see Fig. A-4). Also plotted in Fig. A-4 are the results from the analytical solution (46) for the same notch. It is clear from Fig. A-4 that the value of β:

(i) is a function of K_t and the nominal stress range in the case of elasto-plastic analysis;

(ii) is dependent on K_t but is independent of the nominal stress range in the case of an analytical solution;

(iii) is a strong function of x/A over which regression analysis have been made (see Fig. A-4) for both the elasto-plastic analysis and the analytical solution.

Since β has been found to be dependent on K_t for both the elasto-plastic and the analytical solution, a plot has been drawn between β versus $(K_t - 1)$ (see Fig. A-5). Best fit lines for various aluminum alloys based on elasto-plastic analysis results are shown as a function of the stress range. Similar results for steels (47) also have been shown. Two best fit lines to analytical solutions have been shown as a function of x/A.

Figure A-5 indicates β and $(K_t - 1)$ are related such that:

$$\beta = \alpha(K_t - 1)^{\gamma} \qquad (A\text{-}3)$$

This relationship seems to be independent of the type of solution (analytical or elasto-plastic), stress level and x/A over which regression analysis has been made, and the constant (α) and the exponent (γ) were found to be dependent on the above mentioned variables.

In this study to model the decay of the normalized stress-strain distribution, the functional relationship between β and $(K_t - 1)$ has been fitted to the analytical solution at $x/A = 0.09$ because of its independence on the nominal stress range, so that

$$\beta \approx 1(K_t - 1)^{1.5} \tag{A-4}$$

Therefore, Eq. A-2 becomes

$$\frac{N\left(\frac{x}{A}\right)}{N\left(\frac{\infty}{A}\right)} - 1 = (K_t - 1) \exp - (K_t - 1)^{1.5}\left(\frac{x}{A}\right) \tag{A-5}$$

Figure A-6 shows the comparison between the prediction and the analytical solution for a specimen having infinite width with a circular hole ($K_t = 3$). Thus, Eq. A-5 provides a simple means to study the normalized stress-strain distribution ahead of a notch in terms of K_t for the specimens with infinite widths.

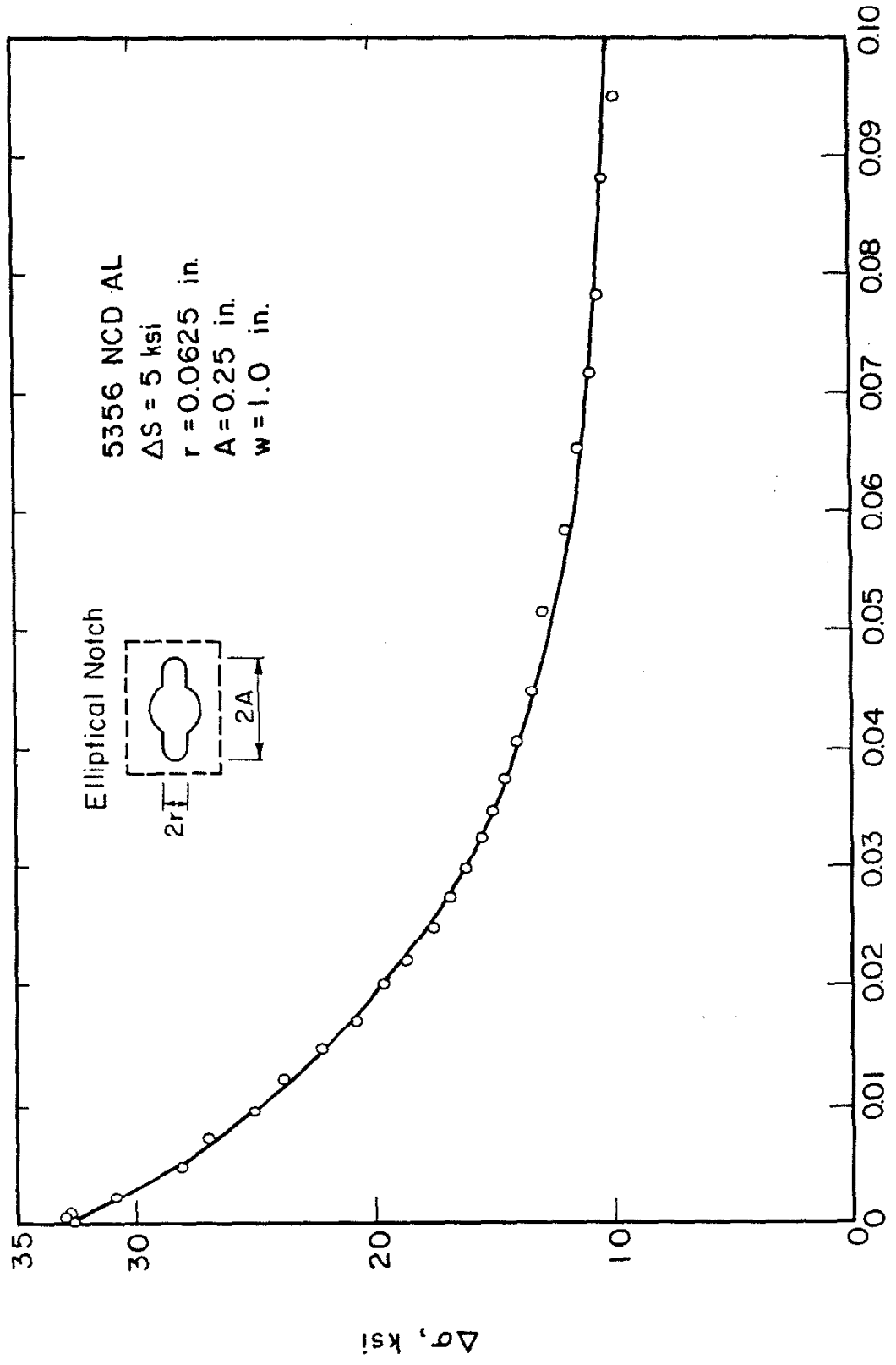

FIG. A-1 STRESS DISTRIBUTION AHEAD OF A NOTCH ROOT IN AN ELLIPTICALLY NOTCHED 5356 ALUMINUM ALLOY SPECIMEN BASED ON AN ELASTO-PLASTIC FINITE ELEMENT ANALYSIS

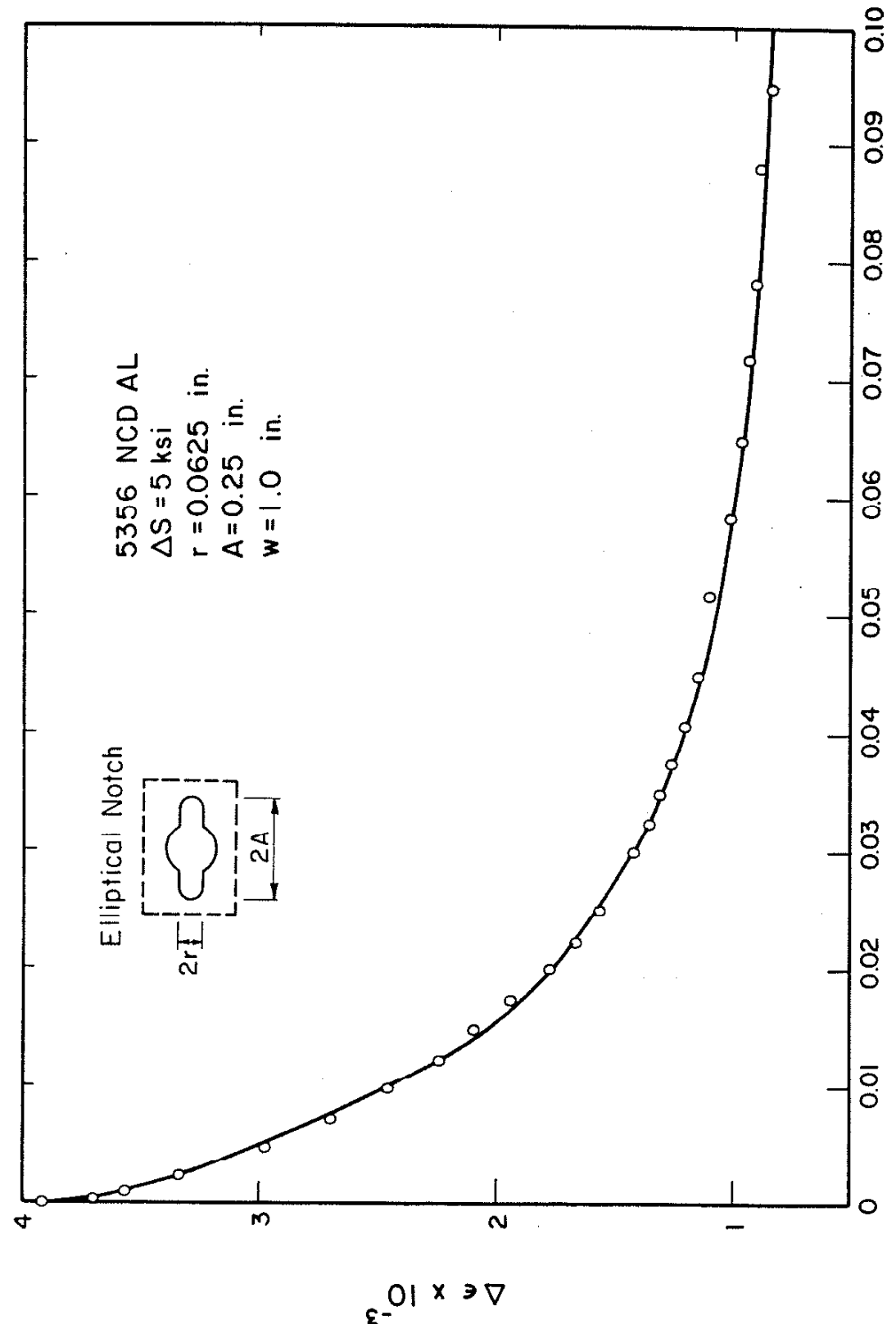

FIG. A-2 STRAIN DISTRIBUTION AHEAD OF A NOTCH ROOT IN AN ELLIPTICALLY NOTCHED 5356 ALUMINUM ALLOY SPECIMEN BASED ON AN ELASTO-PLASTIC FINITE ELEMENT ANALYSIS

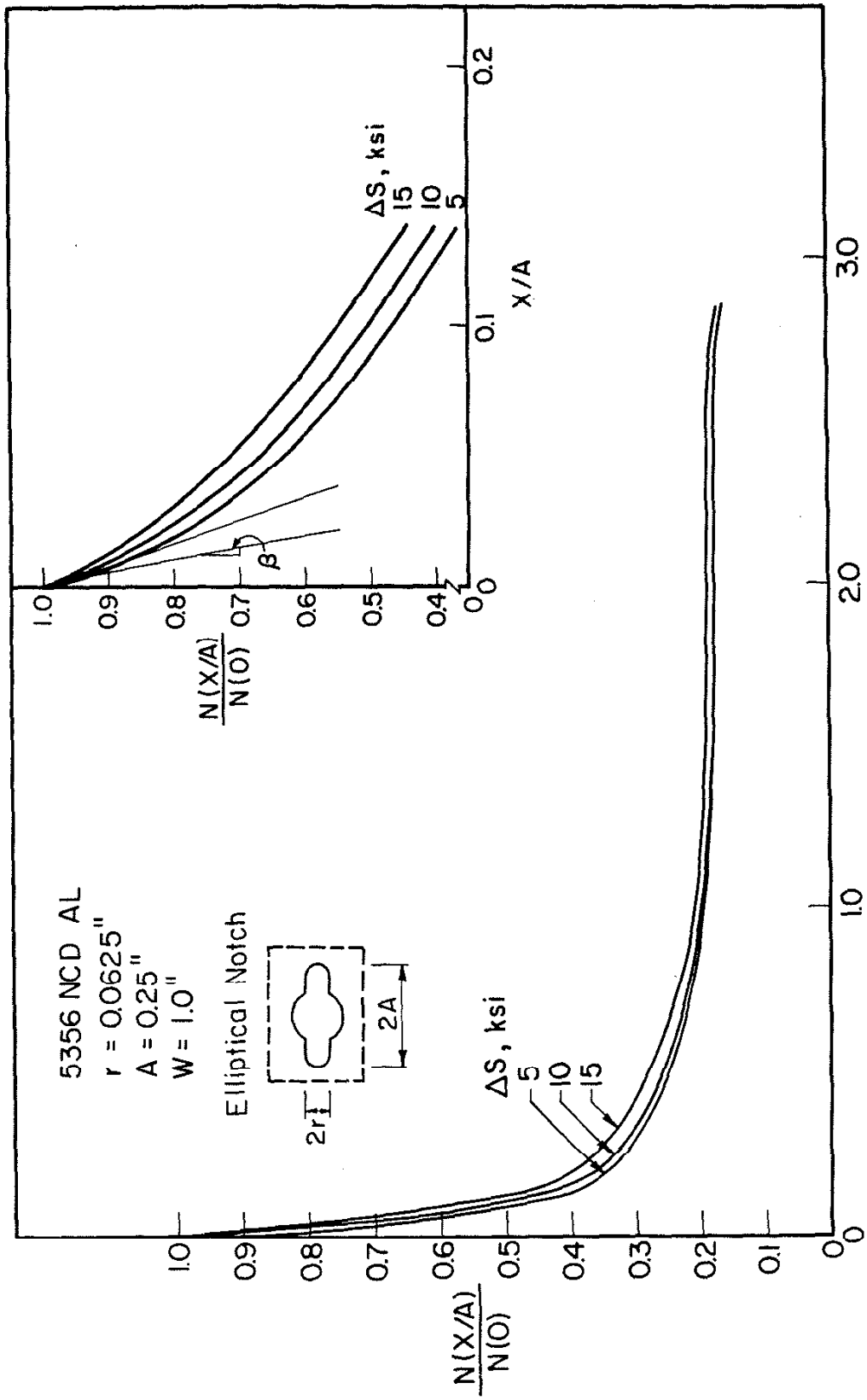

FIG. A-3 NORMALIZED PRODUCT OF THE STRESS-STRAIN DISTRIBUTION AHEAD OF A NOTCH-ROOT FOR AN ELLIPTICALLY NOTCHED 5356 ALUMINUM ALLOY SPECIMEN AS A FUNCTION OF NOMINAL STRESS RANGE

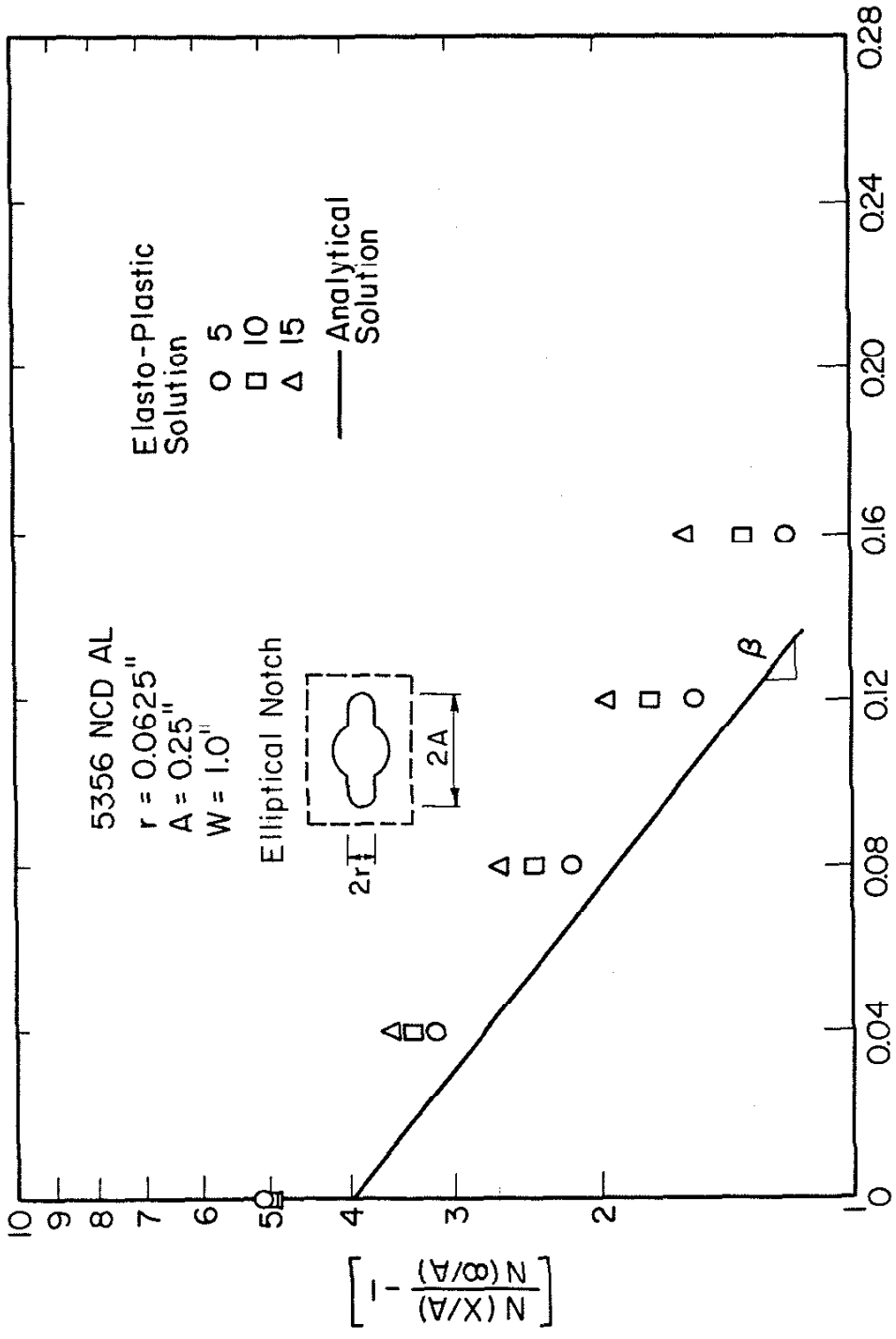

FIG. A-4 CONCEPT OF EVALUATING β

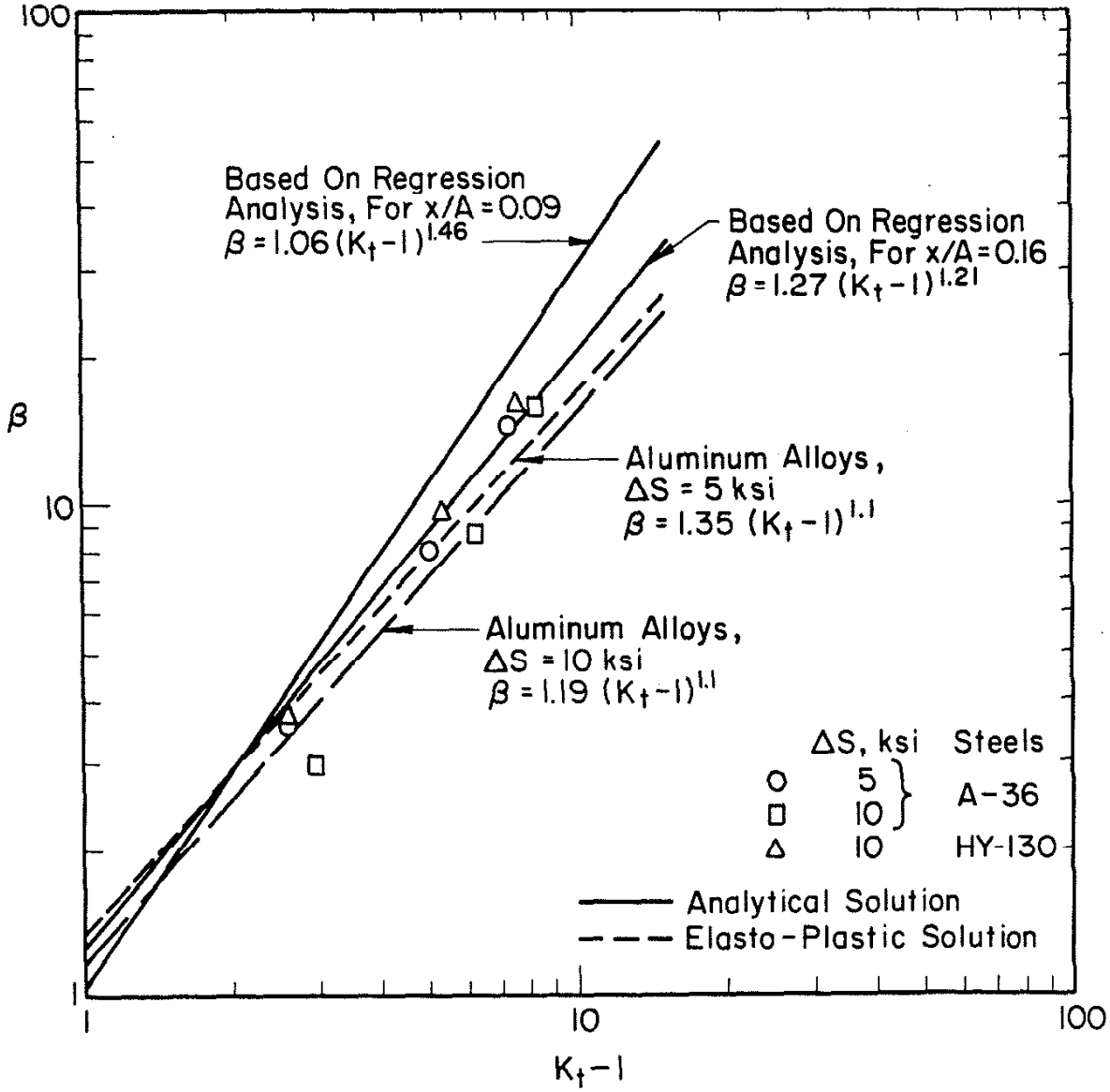

FIG. A-5 VARIATION OF β AS A FUNCTION (K_t - 1) FOR BOTH THE ELASTO-PLASTIC FINITE ELEMENT ANALYSIS OF VARIOUS ALUMINUM ALLOYS AND STEELS

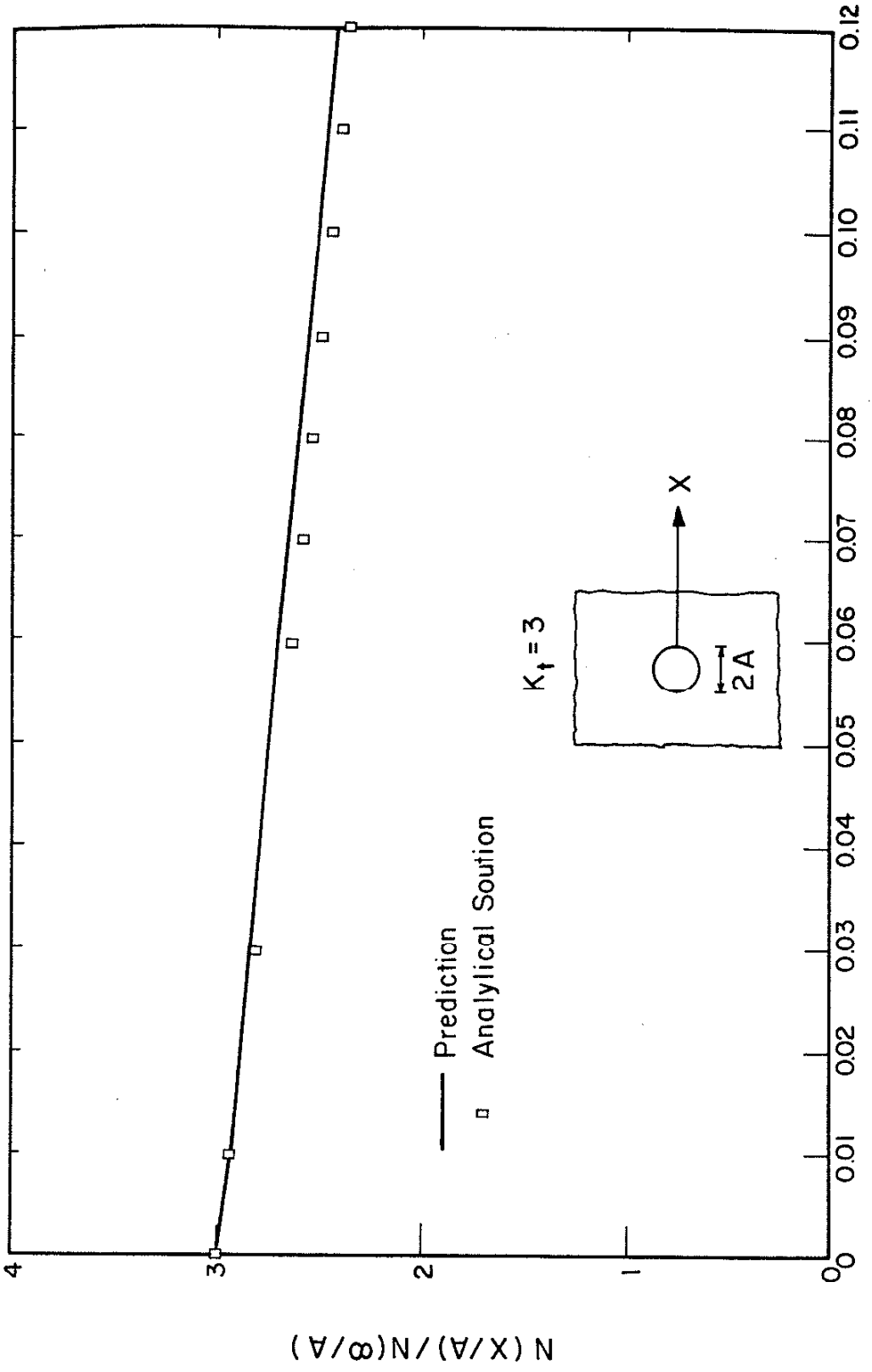

FIG. A-6 COMPARISON OF THE PREDICTED STRESS-STRAIN DISTRIBUTION USING EQ. A-5 WITH THE ANALYTICAL SOLUTION FOR A HOLE IN AN INFINITE PLATE FROM REF. 48